ASC 74-F-015 NASA CR-143692

(NASA-CR-143692) EXPLANATION OF THE COMPUTER LISTINGS OF FARADAY FACTORS FOR INTASAT USERS (Atlantic Science Corp., Indialantic, Fla.) 47 p HC $3.75 CSCL 03B
N75-18138
Unclas
G3/90 11048

EXPLANATION OF THE COMPUTER LISTINGS OF FARADAY FACTORS FOR INTASAT USERS

Prepared by:

G. Nesterczuk
S. K. Llewellyn
R. B. Bent
P. E. Schmid*

Atlantic Science Corporation
P. O. Box 3201
Indialantic Florida 32903

Prepared for:
*National Aeronautics and Space Administration
Goddard Space Flight Center
Greenbelt Maryland 20771

Contract Number: NAS5-21972

November, 1974

TABLE OF CONTENTS

		Page
1.	Computation of the $\overline{M}$ Factor	1
2.	Computer Listing of the $\overline{M}$ Factor	2
3.	Variation of the Faraday Factor	3
Appendix A.	Description of the Bent Ionospheric Model	19
Appendix B.	Earth's Magnetic Field Model	43
Appendix C.	Sample Computer Listing	44

1. Computation of the $\overline{M}$ Factor

Faraday rotation measurements between station and satellite are affected by both the earth's magnetic field and the ionosphere, but can be reduced with the aid of proper conversion factors to a measure of the ionosphere alone. The INTASAT satellite transmits plane-polarized signals at 40.01000 and 40.01025 MHz. These frequencies are much higher than the electron collision frequency and the gyro- and plasma frequencies in the ionosphere; thus, a 'quasi-longitudinal' approximation will hold for propagation in all directions making angles of less than about 89.5° with the earth's magnetic field. Using a simplified form of the Appleton-Hartree formula for the phase refractive index, a relationship can be obtained between the Faraday rotation angle along the angular path and the total electron content along the vertical path, intersecting the angular at the height of maximum electron density.

$$\Omega = \frac{K}{f^2} \int_0^{s_u} B \cos\theta \, N ds = \frac{K}{f^2} \int_0^{h_u} B \cos\theta \sec\chi \, N dh \qquad (1)$$

Ω = Faraday rotation angle in degrees

K = 1.699 = constant

f = signal frequency in hertz

B = earth's magnetic field strength in ampere-turns/m

θ = angle between direction of propagation and earth's magnetic field

χ = zenith angle

N = electron density in electrons/m^3

s = path length in m

h = height above surface of earth in m

h_u= upper integration limit is the height of the INTASAT satellite

Using the second mean value theorem of integration, the function $B \cos\theta \sec\chi$ is removed from under the integral sign and replaced by a 'mean' value.

$$\Omega = \frac{K}{f^2} \overline{M} \int_0^{h_u} N dh = \frac{K}{f^2} \overline{M} N_T \qquad (2)$$

$\overline{M}$ = 'mean' value of ($B \cos \theta \sec \chi$) in ampere-turns/m

N_T = vertical total electron content in electrons/m^2 column

The conversion factor $\overline{M}$ is obtained from both of the above expressions for Ω as,

$$\overline{M} = \frac{\int_0^{h_u} B \cos \theta \sec \chi \, N dh}{\int_0^{h_u} N dh} \qquad (3)$$

The integrals are evaluated in computer mode by generating the electron density N and the function ($B \cos \theta \sec \chi N$) at various height intervals and numerically integrating by Gaussian quadrature. The electron density at each height h is calculated by the worldwide Bent Ionospheric profile model (Reference 1 &2) Each parabolic and exponential segment of the profile was integrated separately with a varying number of points to achieve maximum accuracy. A total of 23 points was used to evaluate the integrals defined in equation (3). The components of the magnetic field strength are obtained by a spherical harmonic analysis routine as described in Appendix B. The assumption of straight line propagation through a spherically stratified ionosphere was made. No bending corrections were calculated as this would have required a prohibitive amount of computer time. At the INTASAT frequencies, bending is a second order effect. Given the straight line propagation assumption the zenith angle at each height h then becomes a function of the ground elevation angle, and the angle θ is calculated using the station and satellite positions and the direction of the magnetic field.

2. Computer Listing of the $\overline{M}$ Factor

The $\overline{M}$ factors are printed on the computer listing for 39 station receiving signals from the INTASAT satellite during the specified time period. The data is sorted by station and date.

For each day the visible satellite passes are numbered sequentially starting at one. If the satellite is continuously visible past 24 hours, the last pass of the first day will only be partial. However, the first pass of the following day will list the complete pass, repeating the data from the first day and flagging the time column by * to indicate the day change. The Greenwich Mean Time for each day runs from 0 hours 0 minutes 0 seconds to 23 hours 59 minutes 59 seconds. Time values of 23:59:59.5 or greater, but less than 24:00:00 are rounded to 24:00:00.

The ionospheric pierce point is printed as the latitude and longitude at which the angular ray passes through the maximum electron density along the path. At this location, the ionospheric profile is computed by the Bent model as required for the computation of $\overline{M}$. The $\overline{M}$ factors are listed in units of ampere-turns/m, and related to Gauss units by 1 Gauss = 79.58 ampere-turns/m. If the $\overline{M}$ value is flagged by **, the angle θ between the direction of propagation and the magnetic field has obtained values between $89.5° \leq \theta \leq 90.5°$, for which the equation relating the Faraday rotation and the total electron content is no longer valid. If this condition occurs above 1000 km, an estimate for $\overline{M}$ is computed using the same equation; if the condition occurs below 1000 km, however, $\overline{M}$ is not computed and a zero value is printed.

Total vertical electron content N_T (el/m^2) is reduced from the Faraday rotation measurement Ω (deg.) using the $\overline{M}$ factor (amp-turns/m) by,

$$N_T = \frac{K\Omega}{f^2 \overline{M}}, \qquad (4)$$

where f is the signal frequency (Hz) and K=1.699 is a constant. An example of the computer listing is given in Appendix C.

3. Variation of the Faraday Factor

A number of graphs are included to demonstrate the variation of the Faraday factor with local time and season, with magnetic latitude, elevation and azimuth angles. The effect of typical day to day fluctuations on the Faraday factor due to sudden increase and decrease in the ionospheric density and height are shown as well as the changes in the angle between the direction of propagation and the magnetic field lines.

As frequently used for convenience, the Faraday factor F in the Figures is the quantity computed from,

$$N_T \ (e/m^2) = F\Omega(\text{degrees}), \tag{5}$$

giving the direct conversion for the angular measurement to the vertical content for a signal frequency f=137 MHz. The relationship to $\overline{M}$ is given by,

$$\overline{M} \ (\text{amp.-turns}/m) = \frac{f^2}{KF} = \frac{1.105 \times 10^{16}}{F(1/m^2 \text{degrees})}. \tag{6}$$

Figures 1 through 5 point out the importance for modeling the Faraday factors correctly with respect to the station position, where the magnetic latitude is of most significance, and with respect to the direction of observation, since the elevation and azimuth angles determine the direction at which the magnetic field lines are intersected as well as the location at which the wave passes through the densest part of the ionosphere. Less important are the specific season and diurnal influences producing variations of only about 2 to 6% in the Faraday factors, as well as the day to day prediction errors in f_oF2 having even less effect. However, prediction errors in ionospheric height which could easily be caused by sudden day to day changes, can have a significant influence on the Faraday factors especially for observations along angular paths. Variations of $\pm$ 100 km in height are not uncommon particularly in the equatorial region. Errors of 5% in the Faraday factor are typical for paths at vertical incidence, but as shown in Figure 3b. for angular paths errors of around 30% in the Faraday factor might occur resulting in proportionally large errors in N_T, since $N_T = F\Omega$. The predicted values of the height of maximum electron density obtained from the Bent model are on average within the accuracy of the measured values, which considering instrumental and reduction techniques, are about 15 km. However, the day to day variations are quite a bit larger, and on occasion, deviations in the predictions of 100 km from the height measurements have been noted.

For a number of stations and observation angles Figures 6a-e. demonstrate the behavior of the angle θ between the direction of propagation and the earth's magnetic field lines between heights of 100 and 1000 km. For fixed station positions and elevation angles the θ angle versus height curves are shown for various azimuth directions. When the condition $89.5° \leq \theta \leq 90.5°$ occurs, the equation relating the Faraday rotation angle and vertical electron content no longer holds true. When θ passes through 90° at a certain height, the wave experiences rotation of the polarization vector in one direction from the satellite down to that height, and rotation in the opposite direction below that height. Contributions to the rotation of the polarization vector in reversed directions cancel out, thus the measurement is not representative of the ionosphere between the satellite and the station.

Acknowledgements

The development and verification of the Bent Ionospheric Model has been supported by the National Aeronautics & Space Administration (NASA) Goddard Space Flight Center Contract No. NAS5-11730; by the U. S. Air Force Space and Missile Systems Organization Contract No. F04701-72-C-0380; and by Air Force Cambridge Research Labs. Contract No. F04701-73-C-0207.

References

1. See Appendix A.

2. R. B. Bent, S. K. Llewellyn, "Documentation and Description of the Bent Ionospheric Model", AFCRL-TR-73-0657, SAMSO-TR-73-252, July 1973.

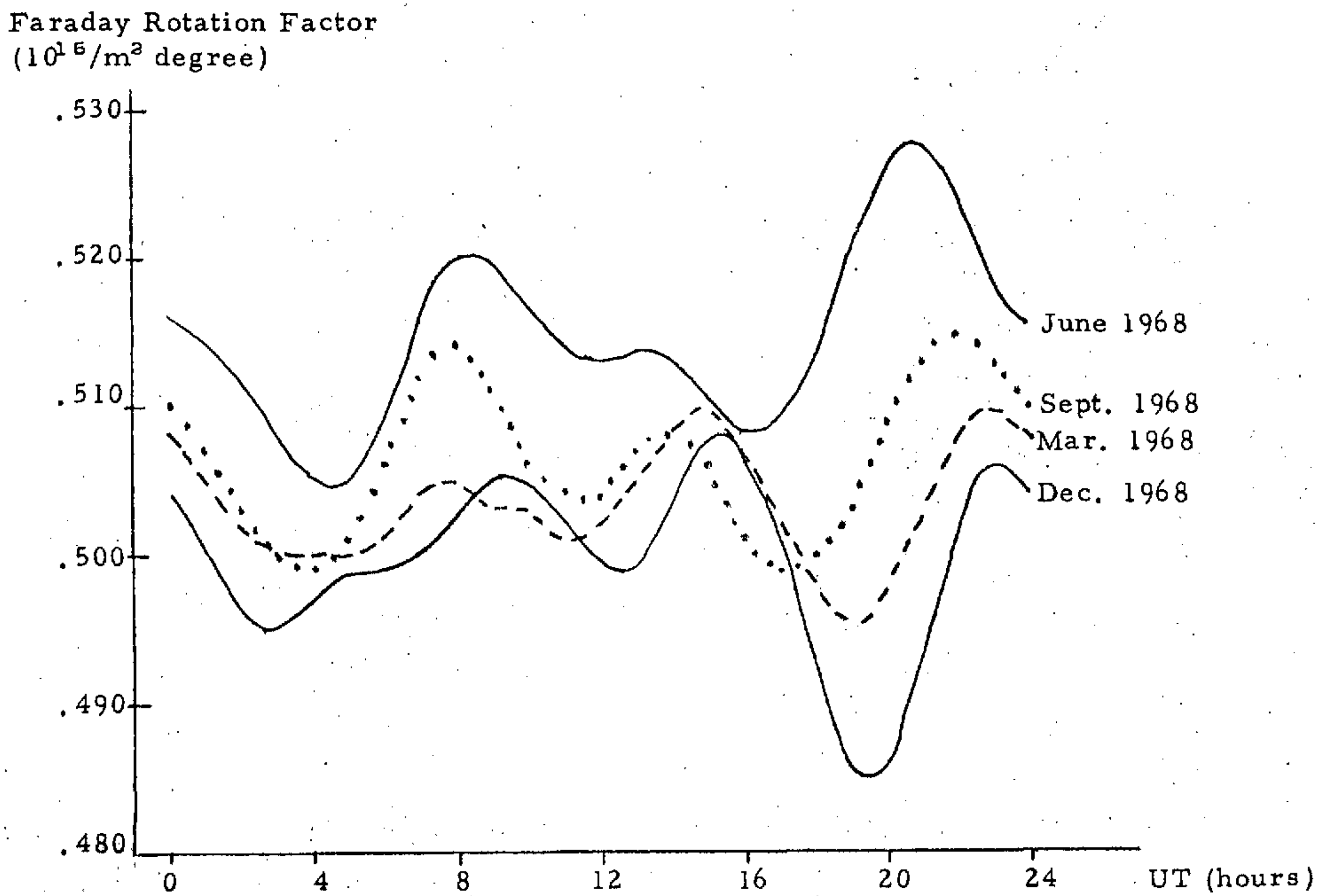

Figure 1. Seasonal and Diurnal Variation of the Faraday Factor F (equation (6)) for Honolulu Looking at an Elevation and Azimuth of 63.6° and 159.3°.

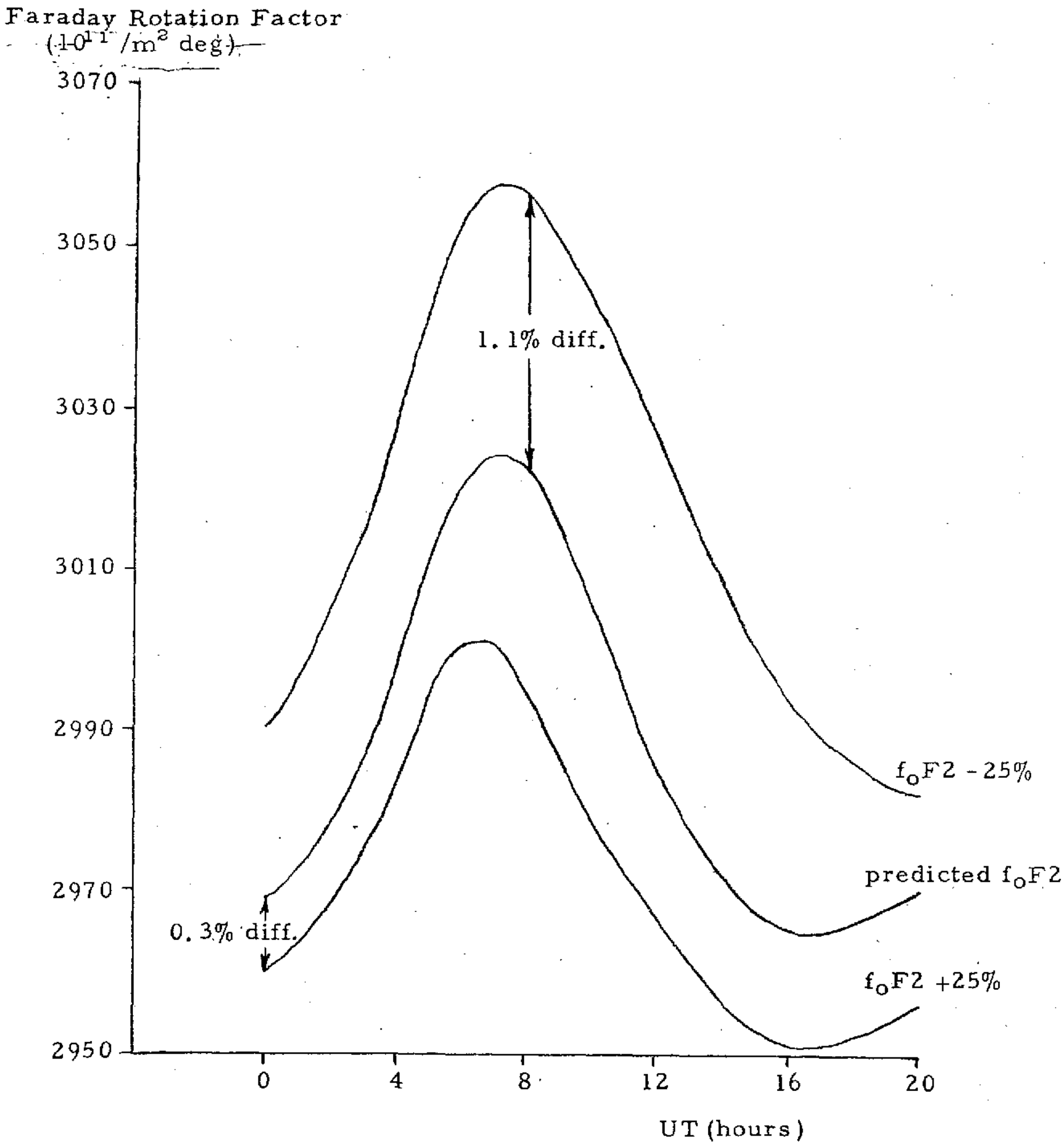

Figure 2. Effect of Increase and Decrease in f_oF2 on the Faraday Factor for a Vertical Path. Station Position = 68.6°, 279.4°, Date = 16 March 1967.

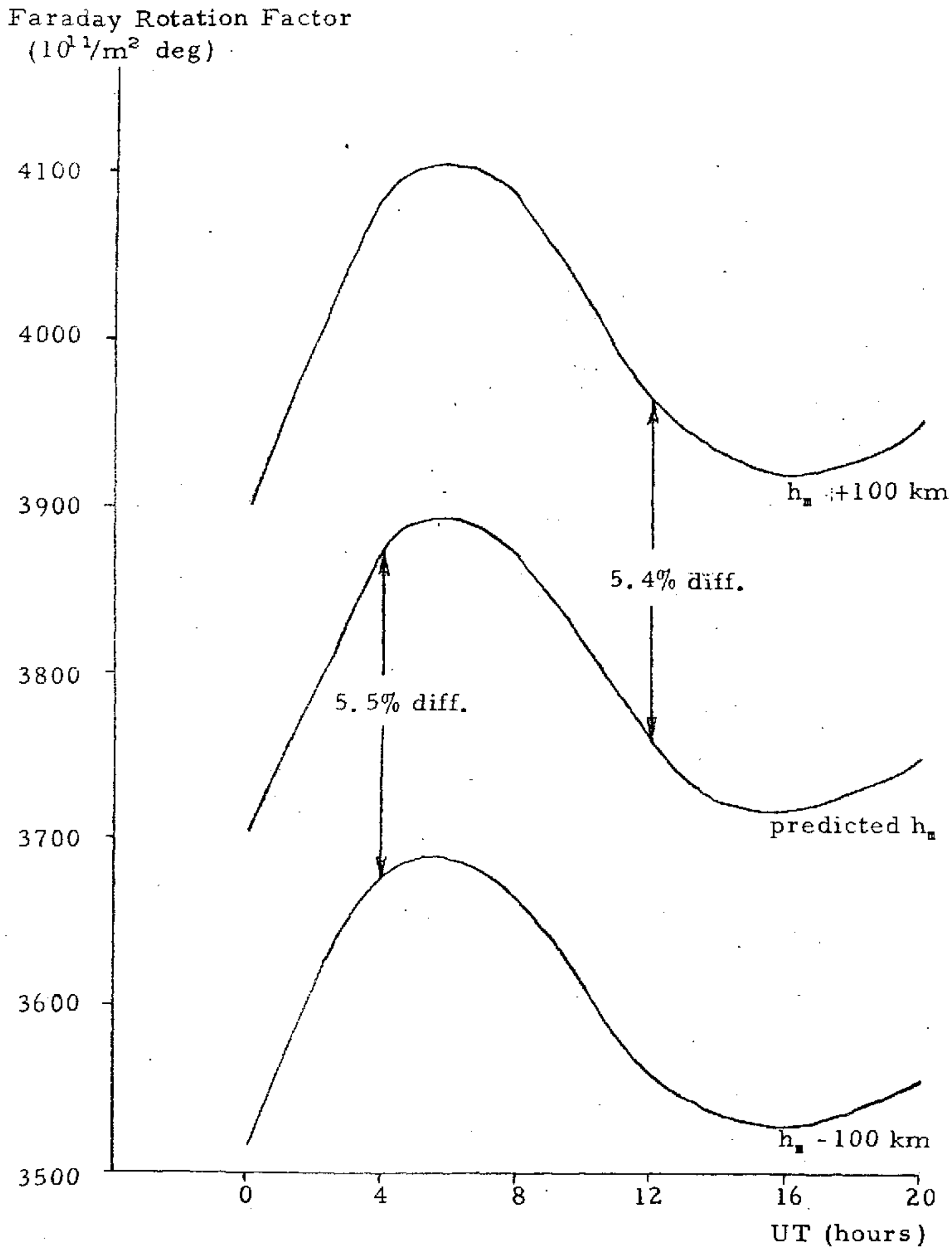

Figure 3a. Effect of Increase and Decrease in the Ionospheric Height on the Faraday Factor for a Vertical Path. Station Position = 28.6°, 279.4°, Date=16 March 1967.

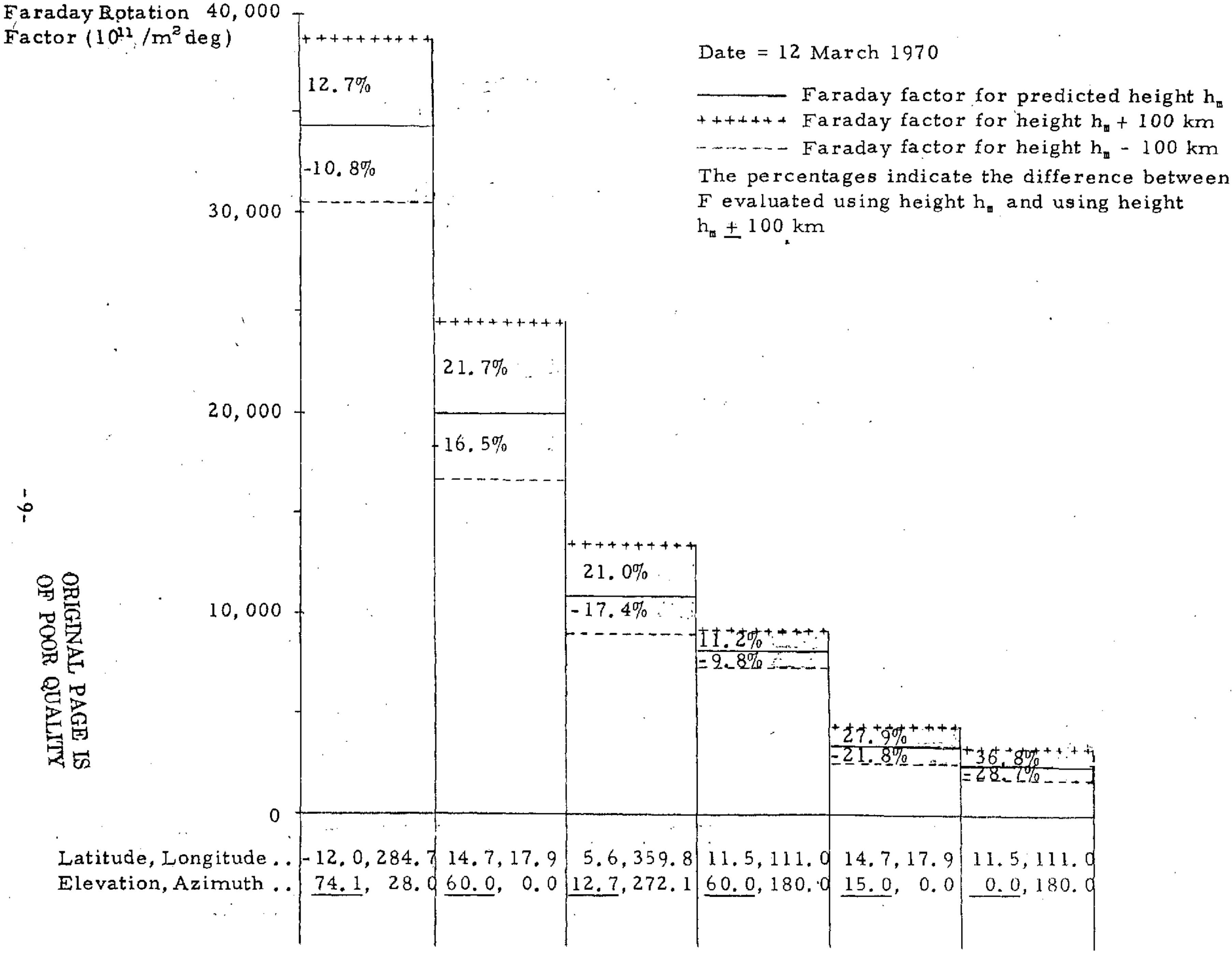

FIGURE 3b. Effect of Variation in Ionospheric Height on the Faraday Factor F for an Angular Path

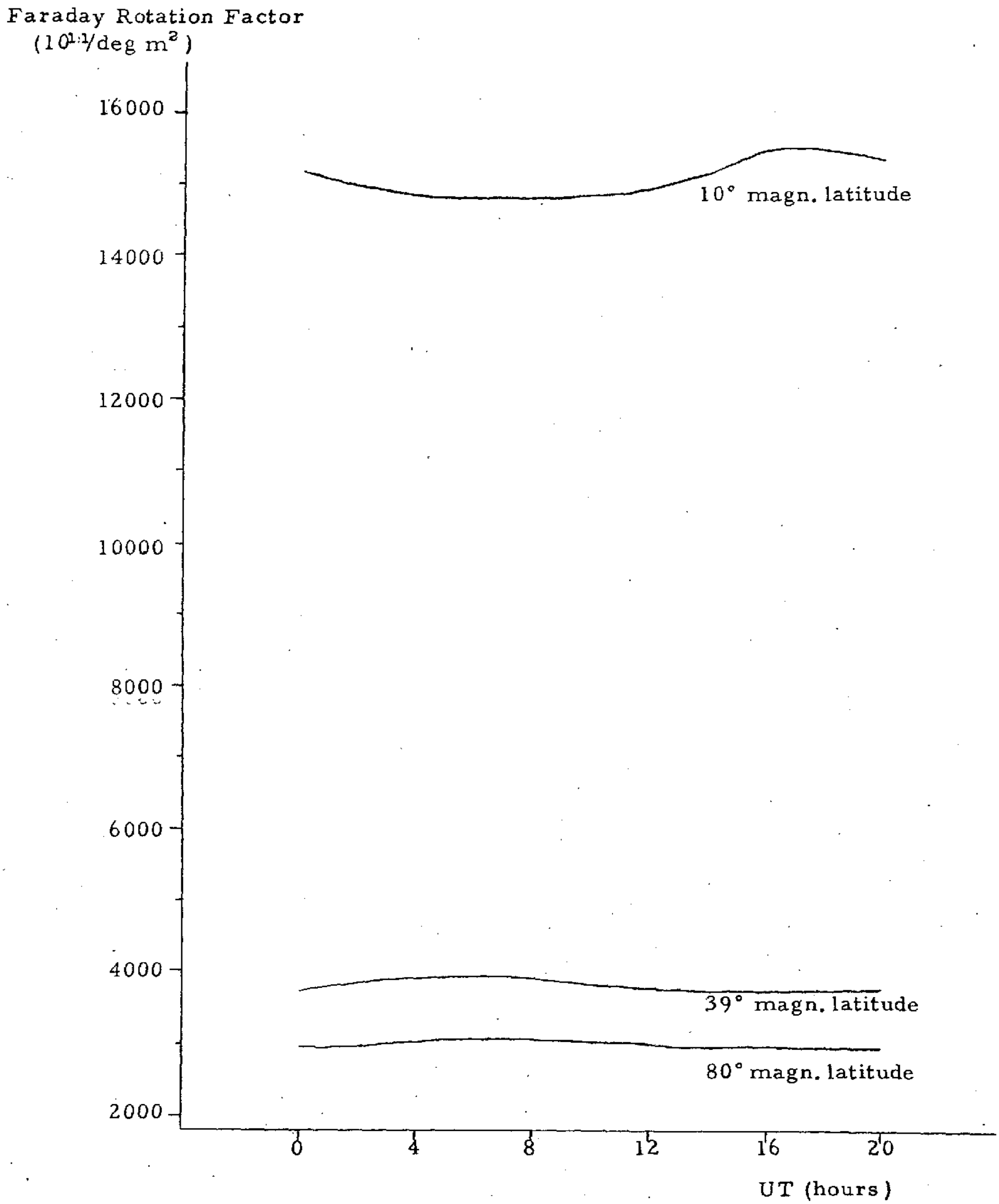

Figure 4. Variation of the Faraday Factor with Magnetic Latitude for a Vertical Path and with the Diurnal Changes on 16 March 1967.

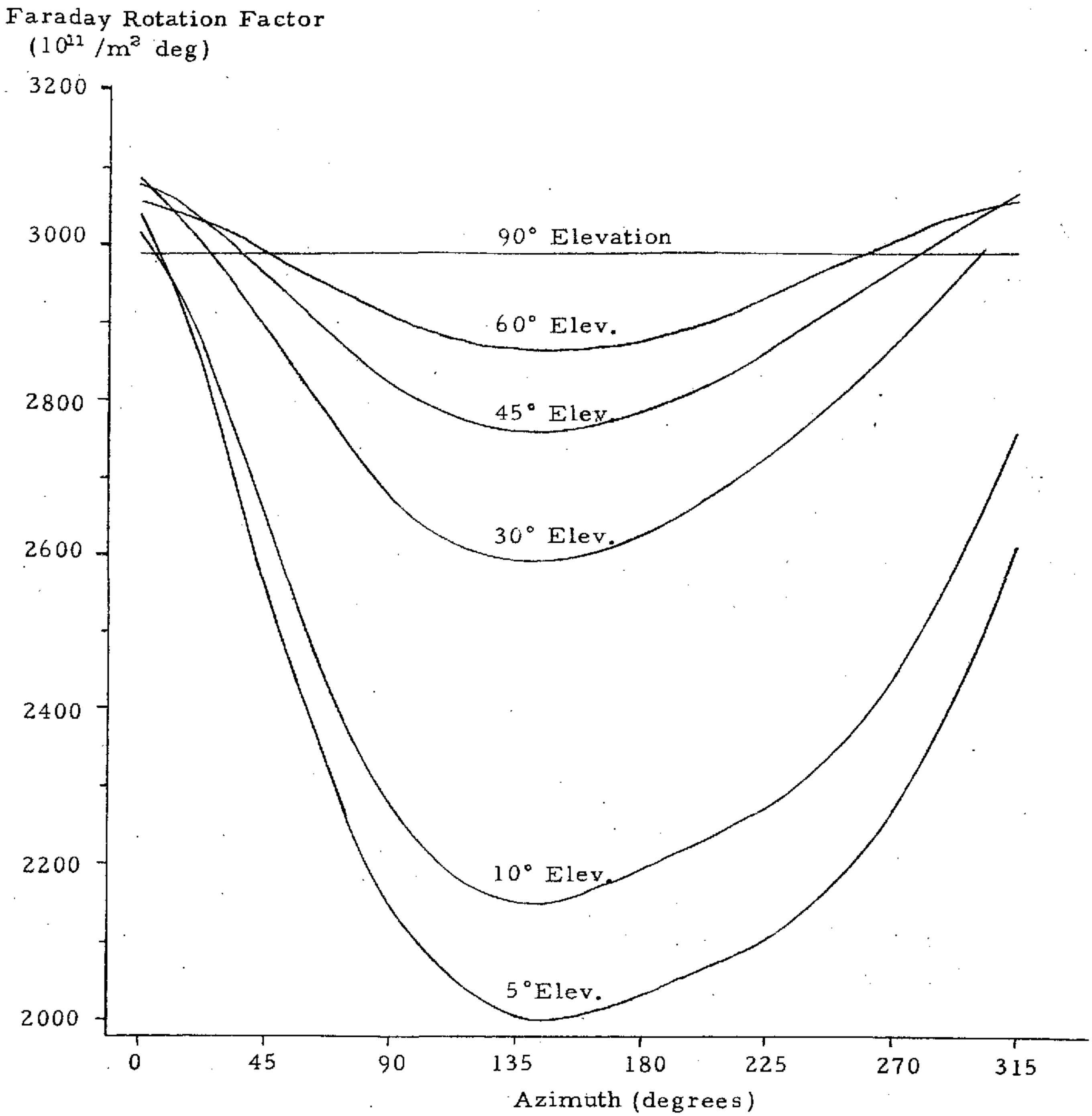

Figure 5a. Variation of the Faraday Factor with Changes in Elevation and Azimuth Angles at 80° Magnetic Latitude.
Station Position = 68.6°, 279.4°, Date = 16 March 1967, UT=12 hours.

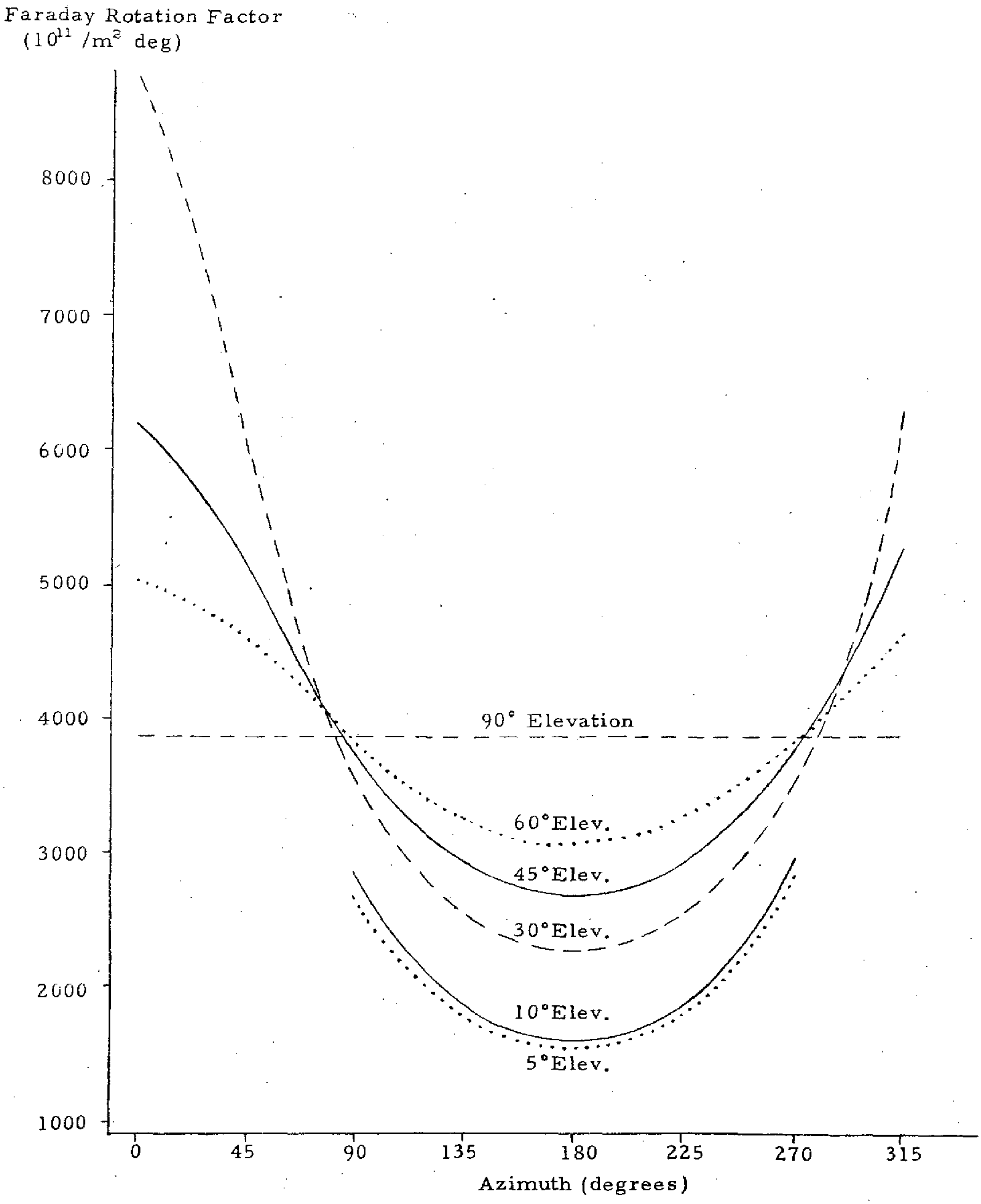

Figure 5b. Variation of the Faraday Factor with Changes in Elevation and Azimuth Angles at 39° Magnetic Latitude. Station Position=28.6°, 279.4°, Date=16 March 1967, UT=11 hours.

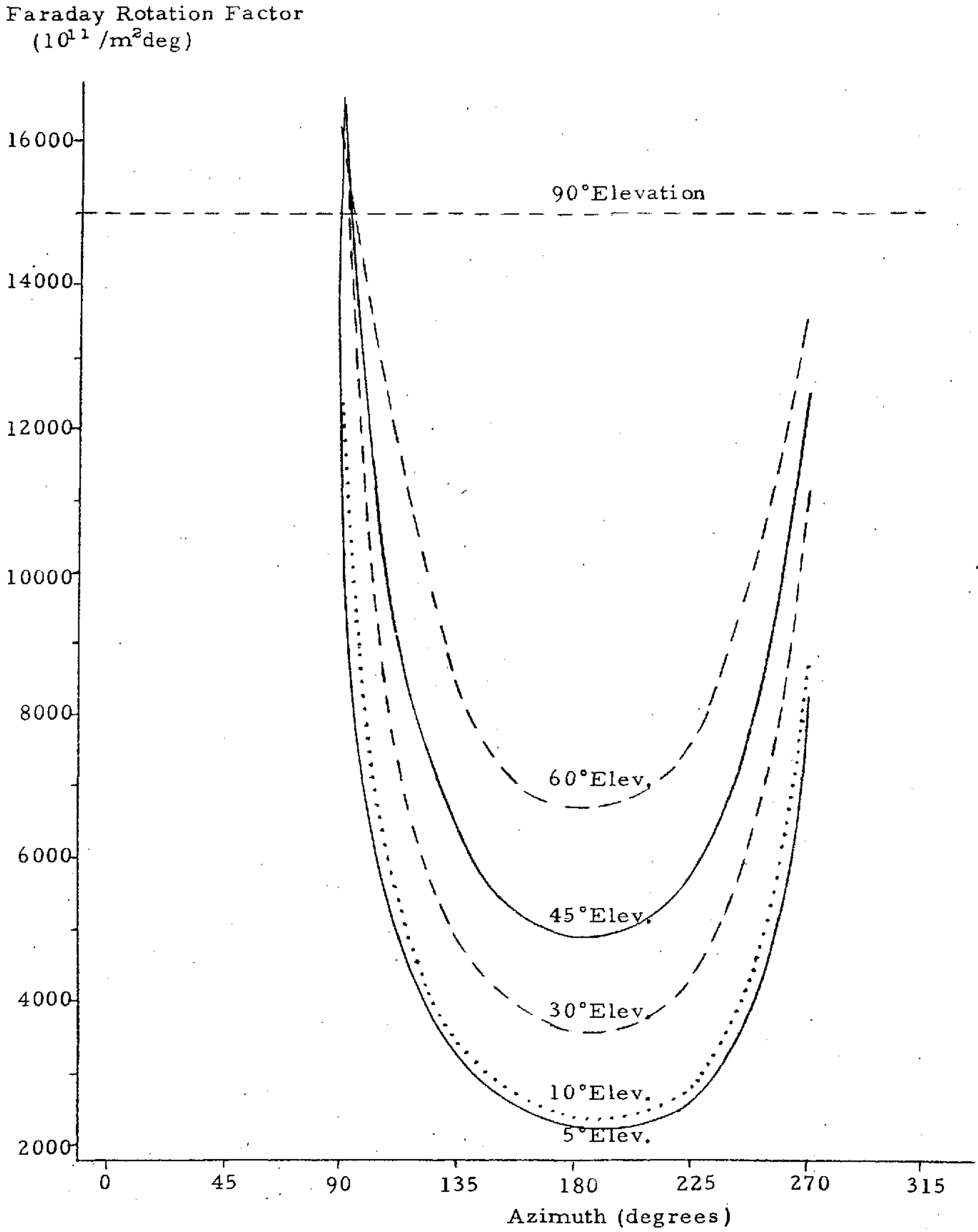

Figure 5c. Variation of the Faraday Factor with Changes in Elevation and Azimuth Angles at 10° Magnetic Latitude.
Station Position = -1.2°, 279.4°, Date = 16 Mar 1967, UT=14 hours.

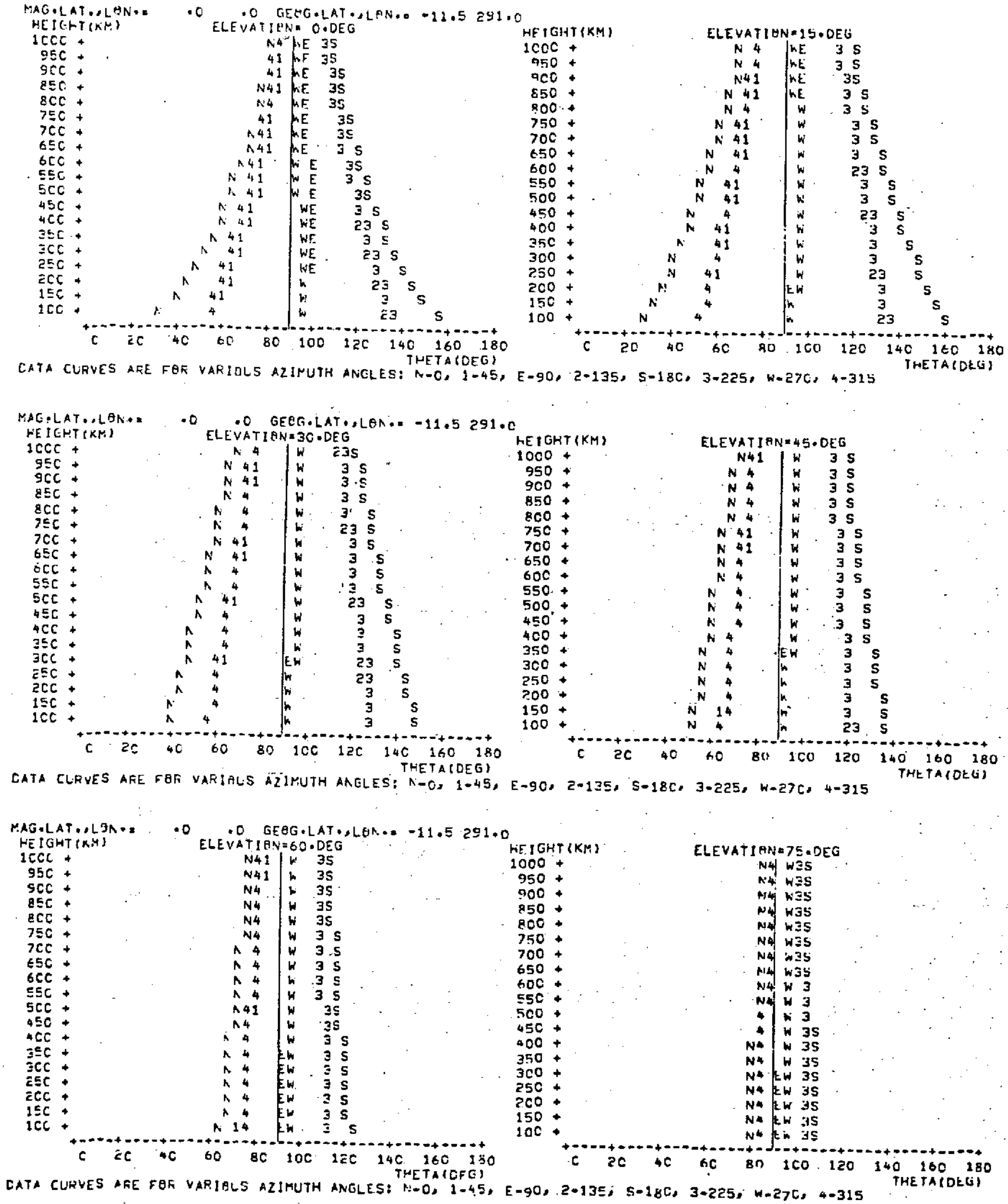

Figure 6a. Variation of the Angle θ Between the Direction of Propagation and the Magnetic Field

ORIGINAL PAGE IS
OF POOR QUALITY

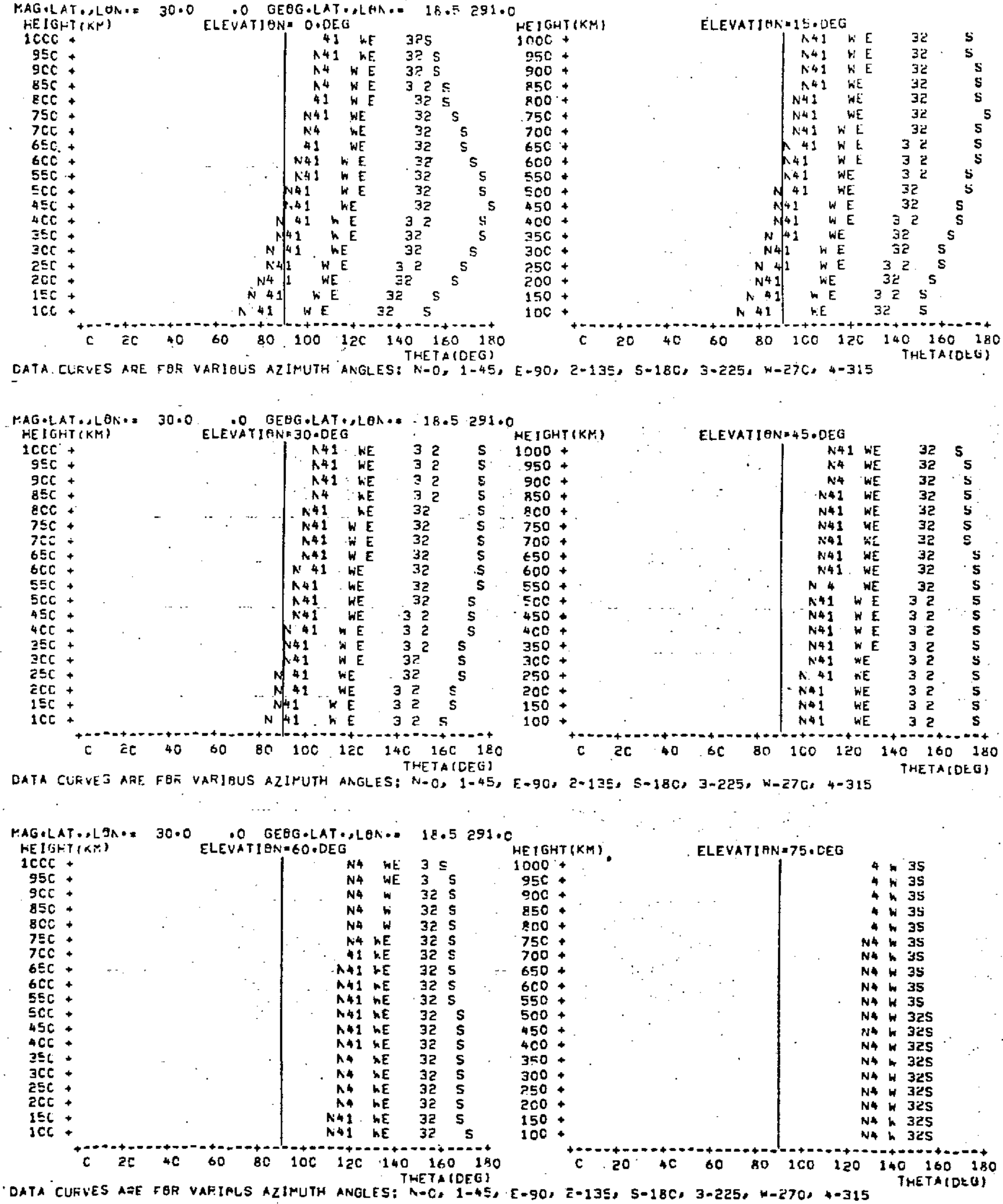

Figure 6b. Variation of the Angle θ Between the Direction of Propagation and the Magnetic Field

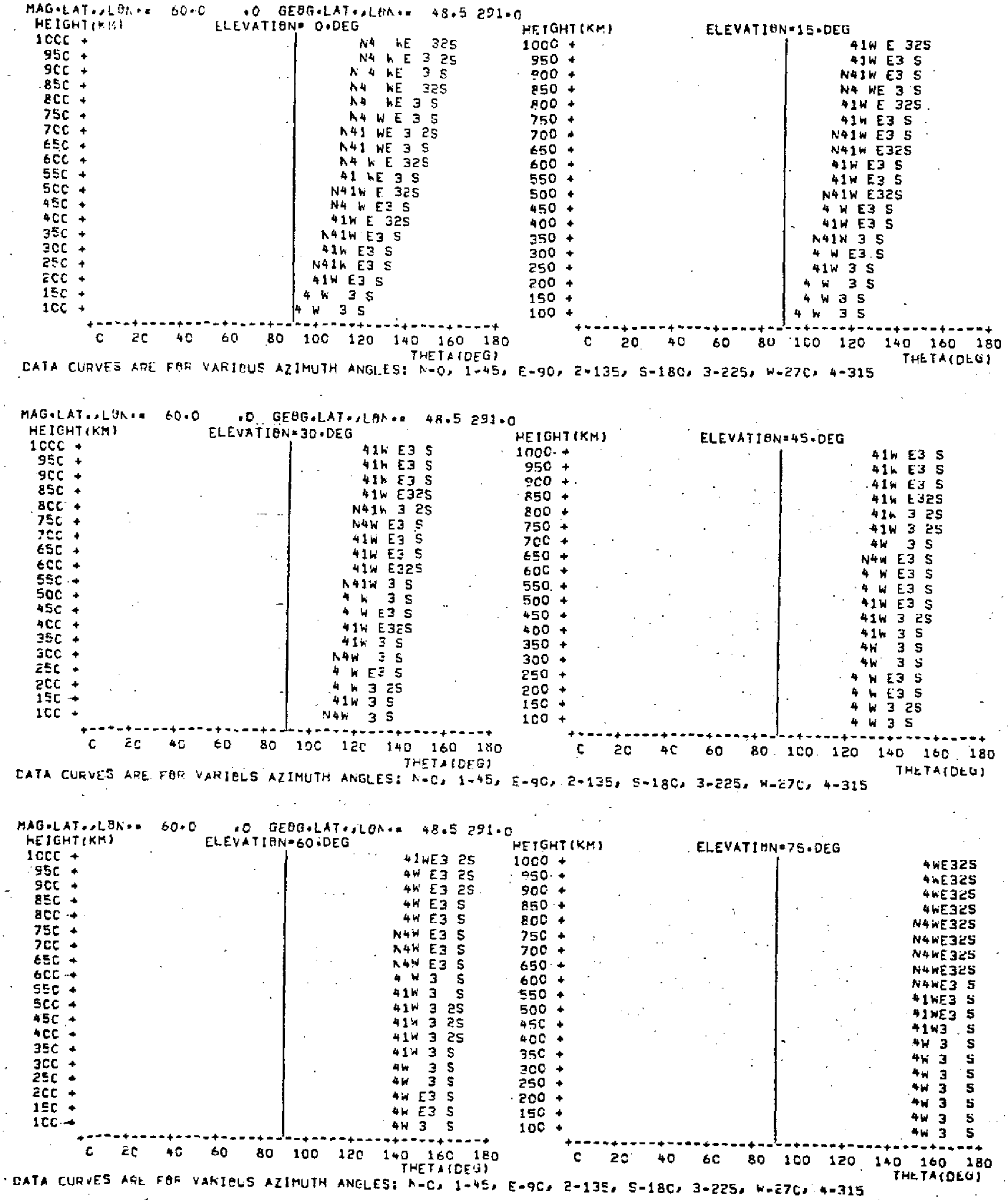

Figure 6c. Variation of the Angle θ Between the Direction of Propagation and the Magnetic Field

ORIGINAL PAGE IS OF POOR QUALITY

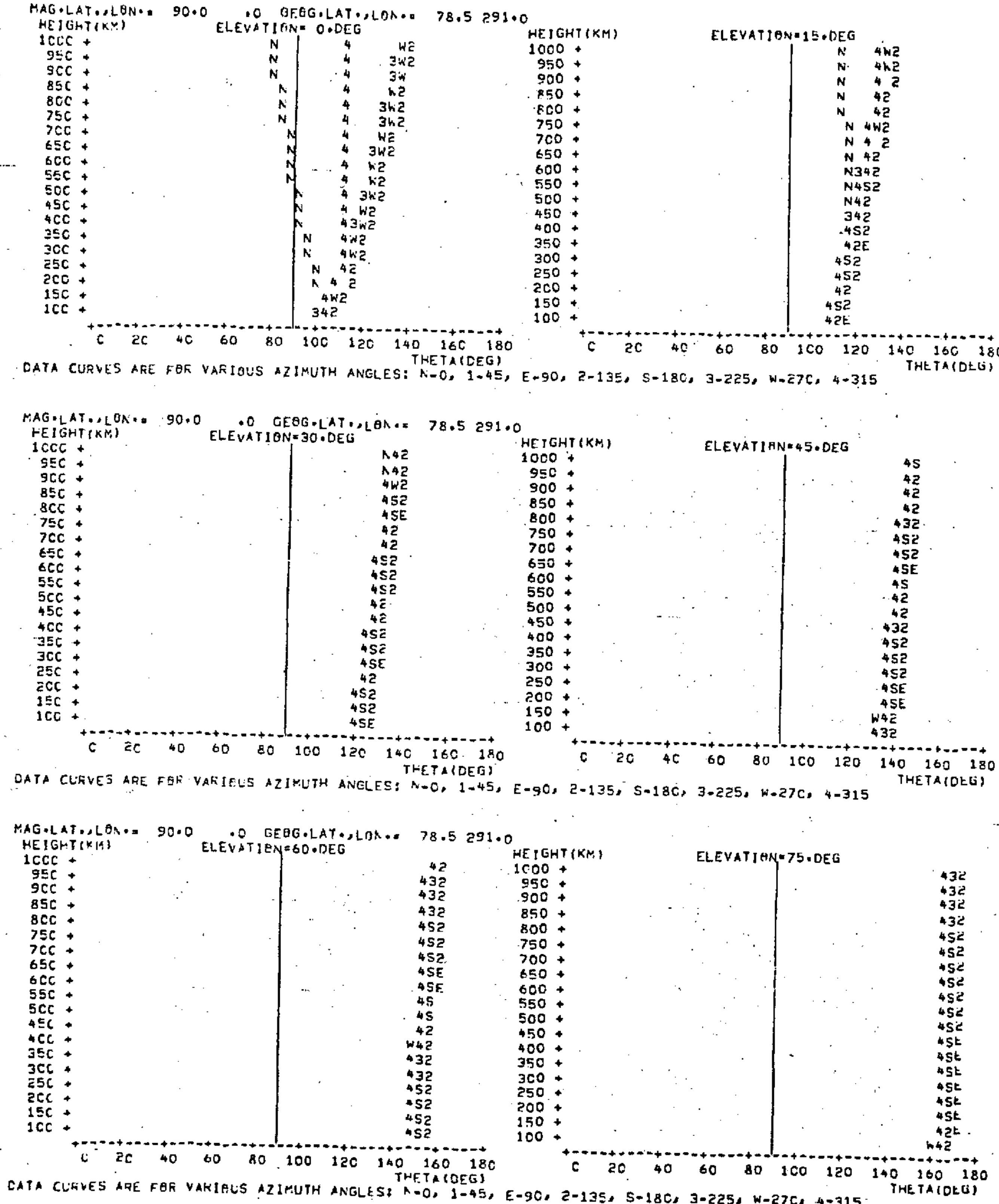

Figure 6d. Variation of the Angle θ Between the Direction of Propagation and the Magnetic Field

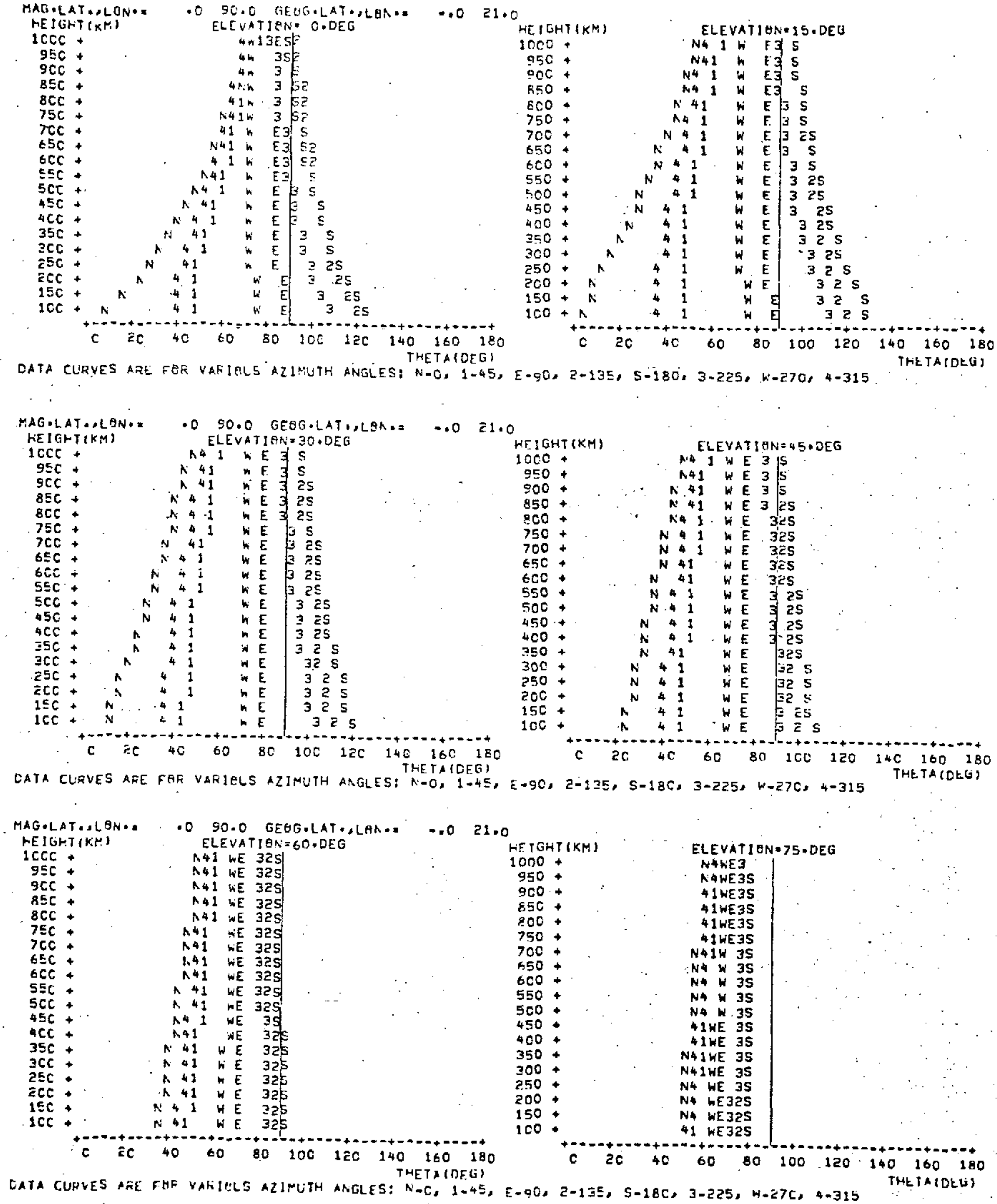

Figure 6e. Variation of the Angle θ Between the Direction of Propagation and the Magnetic Field

APPENDIX A

DESCRIPTION OF THE BENT IONOSPHERIC MODEL

A.1 Ionospheric Model Development

For several years scientists have investigated many different approaches to modeling the ionospheric profile on a theoretical basis. The names and types of these methods are well known and will not be discussed here, but it is obvious after all the years that a good theoretical ionospheric profile still does not exist.

The object of our past investigations was to come up with an ionospheric profile that could give much improved results for refraction corrections in satellite communications to ground or to another satellite than had been obtained with the Chapman and many other theoretical profiles. It would have been pointless for us to sit down and investigate another theoretical approach when so many more competent scientists are working on this problem. For this reason we decided that in this present time of computers, an empirical model taken from a vast data base may provide us with the profile we were looking for.

It was our intention to acquire ionospheric data of any kind that helped us build up a data base covering minimum to maximum of a solar cycle and providing information up to 1000km. The lower layers of the ionosphere were neglected in terms of their irregularities although their electron content was added into the larger F layer; this was done to simplify the approach and as the prime objective was to obtain refraction corrections through the ionosphere, or at least to a point above 150 km, such an elimination would not be very detrimental.

Data from bottomside ionospheric sounders was obtained over the year 1962 through 1969 covering 14 stations approximately along the American longitudes having geographic latitudes 76 degrees to -12 degrees or magnetic latitudes 85 degrees to 0 degrees. This data was in the form of hourly profiles of the ionosphere up to the f_oF2 peak. Topside soundings were acquired for the years 1962 to 1966 covering the magnetic latitude range 85 degrees to -75 degrees and providing electron density profiles from about 1,000 km down to a height just above maximum electron density. As the topside data was

ORIGINAL PAGE IS
OF POOR QUALITY

not available near the solar maximum, electron density probe data was obtained from the Ariel 3 satellite over the period May 1967 to April 1968 from 70 degrees north to 70 degrees south geographic latitude and linked in real time to f_oF2 values obtained from 13 stations on the ground.

A.1.1 Ionospheric Profile

In order to analyze the vast amount of data that was obtained a number of assumptions had to be made. In the first case the topside sounding data did not geographically cover the entire globe and the bottomside data was only available for land masses and not over the oceans; however, as a local time effect is far more significant than a longitude effect, the data was analyzed as a function of latitude and local time. Geographic longitude was, however, taken into account for the determination of maximum electron density by using the ITS coefficients for f_oF2 which are a function of latitude, longitude, time and solar activity. Secondly a theoretical profile was determined to which the data would fit. This profile which is used in the evaluation discussed later, is shown in Figure 7 and is the result of earlier work by Kazantsev (Reference 4), and unpublished work of Bent (1967) while at the Radio and Space Research Station in England and requires the knowledge of the parameters k_1, k_2, k_3, y_t, y_m, f_oF2, and h_m. The equation of the upper topside is exponential, namely,

$$N = N_0 e^{-ka},$$

the lower ionosphere is a bi-parabola,

$$N = N_m \left(1 - \frac{b_2^2}{y_m^2}\right)^2,$$

and the top and bottomside are fit together with a parabola,

$$N = N_m \left(1 - \frac{b_1^2}{y_t^2}\right),$$

where,

N	is the electron density
N_m	is the maximum value of electron density
N_0	is the maximum electron density for each exponential layer

a and b are vertical distances

y_m	is the half thickness of the lower layer
y_t	is the half thickness of the upper parabolic layer
k	is the decay constant for an exponential profile.

The upper parabola extends from the height of the maximum electron density up to the point where the slope of the parabola matches the slope of the exponential layer. The data investigated included over 50,000 topside soundings, 6,000 satellite electron density and related f_0F2 measurements, and over 400,000 bottomside soundings.

A.1.2 Topside Ionosphere

The initial approach was to take the topside soundings and break them down into zones 5 degrees of latitude by 40 minutes of local time eliminating data in the same zones that have similar times and profiles, and therefore are duplicated. This resulted in over 1,200 different areas in the northern and southern hemisphere with a reasonably constant density of data in each area. By these means it was possible to investigate the decay constant k in the exponential topside profile as a function of local time, latitude, solar flux, sunspot number and season. One of the major concerns was whether the decay constant k would be uniform for each sounding over the range 1,000 km to the minimum height, and investigations showed that such an exponential profile does not exist. The layer was, therefore, divided into three equal height sections from 1,000 km to the minimum recorded height and the exponent k computed for the center point in each section. Figure 7 shows such a division where the values under investigation are the decay constants k_1, k_2, k_3. In most cases the topside soundings do not reach the height of maximum electron density and therefore the gradient at this lower point was mathematically equated to the point where the gradient of the 'nose' parabola was the same. Extensive analysis of the acquired data showed these gradients to be similar, on average, at a height y_m /4 above the maximum electron density. At this point the value of f_kF2, which defines the lowest point of the topside sounding, is 0.93 f_oF2. (N_o in Figure 7 is the equivalent electron density to the frequency f_kF2).

For an initial test the decay constants k for each of the three layers, upper, middle, and lower topside were plotted as a function of magnetic latitude and f_kF2. Values from the northern and southern hemispheres were treated independently at first, but the analysis showed that there was excellent correlation between the two. Figure 8 shows the relationship between the three decay constants k and magnetic latitude for all local times, solar activity, and season. The equatorial anomaly and a 40 degree trough show in the lower topside layer. The 65 degree trough is not as evident as it is when the same analysis is done for various local times which suggests the physical variances of these anomalies should be investigated in more detail.

It was found that correlations in k for specific f_kF2 did not bear any further local time correlation, but bore a significant variation with solar activity and magnetic latitude. However, the correlation with solar flux was considerably better than that with sunspot number, even allowing for the delay in the effect reaching the ionosphere, so all further correlations were with the Ottowa 10.7 cm solar flux. All these correlations were then plotted in graphical form to enable final interpolation.

Unfortunately the Alouette data did not cover the period at the peak of the solar cycle, but the Director of the U.K. Radio & Space Research Station made available electron density data from the Ariel 3 satellite to cover this period. The data had already been reduced thoroughly and the satellite electron density at about 550 km was provided with the sub-satellite f_oF2 value obtained from 13 stations around the world. If the satellite was not directly over an ionosonde at the time of observation, the f_oF2 values from two or three transmitters in the general area had been interpolated in time and position to give the sub-satellite value. These interpolations had been carried out taking care to modify the values for uneven ionospheric gradients. Data that was in doubt was eliminated. While these values did not give the three exponential decay constants at each point, it was found that for similar conditions of solar flux and position, the Ariel 3 data fit very closely to the profiles deduced from Alouette 1. The profile equations developed for the lower solar activity period related to the topside sounders could, therefore, be extended to the larger solar flux values and still be in good agreement with the Ariel 3 data. Typical results from this analysis are shown in the graphs of Figure 9. The original data curves were less regular, and since the variations were mainly caused by the relatively low data density in each group after division of the large data base, the data was smoothed by the fitting of straight lines. In order to interpret these graphs and obtain a profile, we need the value of f_oF2. and the magnetic latitude position. These values will indicate which graph relates the 10.7 cm flux to the decay constants k for the upper, middle, and lower portions of the topside ionosphere. Figure 9, therefore, shows the basis of obtaining the 3 independent slopes of the topside ionosphere as a function of f_oF2, latitude, and solar flux.

A further correlation to investigate the seasonal effects on k was carried out with some 15,000 totally different Alouette soundings and fluctuations in the k values of $\pm$ 15% were noted from the average spring and autumn values. The seasonal variation is monitored by observing the change in the daily maximum solar zenith angle from the equinoctial mid-day value. Figure 10 shows the seasonal fluctuation in k for each of the three layers in the topside profile. There is considerable evidence that this seasonal relationship has an added local time factor and this point will shortly be under investigation.

Examination of the upper part of the 'nose' of the N-h profile is difficult because topside sounding information rarely gives any values in this region.

Evidence from many leading scientists also implies that the topside profiles have about a +4% error in the effective distance from the sounding satellite indicating the obtained topside profiles are too low near the peak. This evidence is based on comparisons with two-frequency data, backscatter results, Faraday rotation and overlap tests, etc. Preliminary results in this empirical model showed that a parabola in this region gave the better comparison with integrated total electron content when compared with two-frequency and Faraday rotation data. A simple parabola having a half thickness y_t was fitted between the bi-parabola and the exponential layer. Upon initial test y_t was set equal to the half thickness of the bi-parabola y_m for f_oF2 values below 10.5 MHz, and y_t increases with f_oF2 values rising above 10.5 MHz. Further investigations of this problem are planned in future work.

The final step in predicting the shape of the ionosphere is arranging for the gradient in the upper parabolic layer to be the same as the gradient in the lowest part of the topside exponential layer. This is the case at a distance $d = 1/k\,[(1+y_t^2 k^2)^{\frac{1}{2}} - 1]$ above the height of the maximum electron density.

A. 1.3 Bottomside Ionosphere

Modeling the bottomside ionospheric profile was a somewhat easier task because for each profile the value of f_oF2 was known and the electron density versus height profile from h_{min} to h_{max} was also known. Once more the geographic effect of longitude was eliminated and replaced with the more simple local time correlation. From Figure 7 we see that the equation of the lower layer is a parabola squared or a bi-parabola. This was found in general to fit the real profile somewhat better than a simple parabola. The unknown in this equation is the half thickness of the layer y_m and in the reduction of the data the y_m value was treated in a similar way to a topside k value.

The irregularities in the ionosonde data due to the lower layers of the ionosphere were smoothed out because the prime objective of the work was to simplify the model, but keep the total content as accurate as possible. The sounding data was therefore integrated up to the peak electron density (N_m) and forced to fit the bi-parabolic equation along with the value of N_m obtained from the sounding. In each instance the value of y_m was computed ready for further correlation.

A number of real profiles from various stations at different local times were compared with the computed profile and excellent agreement found. A further 12,000 soundings from all 14 stations were analyzed and the computed value of y_m compared to the actual measured value. These results are shown in Figure 11 along with the RMS errors. The two tests indicate that the bi-parabolic profile is, on average, in close agreement to the real profile. Investigations, similar to those carried out for the topside decay constants, correlated y_m with solar flux f_oF2, local time and season. Surprisingly, no direct correlation was found between y_m and solar flux, but a definite correlation existed in local time and also in the solar zenith angle at local noon which represents the season.

Figure 12 indicates how y_m can be determined from local time and f_oF2, and Figure 13 shows the seasonal update as a function of local time for the sunrise, sunset, night and daytime period. In the cases where f_oF2 was larger than 10 MHz the local time curve fluctuated very little from the 10 MHz curve. All of the curves displayed have not been hand smoothed; due to the large data base the average of all values taken every hour fit precisely on the lines shown.

The remaining unknowns which are needed to compute the profile are f_oF2 and the height of that value; by far the most important of these being the value of f_oF2.

A.1.4 Predicting f_oF2

Severe horizontal gradients in f_oF2 exist within the ionosphere as can be seen by examining Figure 14. In fact even if the value of f_oF2 is known directly above a station, it can change considerably over the whole 'visible' ionosphere from that site. Figure 14 is a predicted status of f_oF2 over the world at 6.0 am during August 1968 and two types of severe gradients are immediately noticeable, one due to sunrise causes rapid changes in f_oF2 in an east to west direction and the other situated around the equatorial anomaly occurs primarily during the afternoon and early evening and causes severe gradients in the north to south direction. Two hypothetical stations, A and B, are marked on Figure 14 along with the ionosphere 'visible' from those sites. In case A the value of f_oF2 changes from 11.5 MHz directly overhead to 5 MHz on the southern horizon. This change must be squared when converting to electron content hence a difference of a factor of over 5 in the vertical content arises before correcting for elevation angle effects. Similar gradients exist over half the earth's surface at some time of the day and it is therefore imperative to model these gradients in any ionospheric model.

For many years NOAA (formerly CRPL and ITSA) have been engaged in the development of numerical methods and computer programs for mapping and predicting characteristics of the ionosphere used in telecommunications. The most advanced method for producing an f_oF2 model undoubtedly comes from their work. Jones, Graham & Leftin (Reference 2) describe their techniques on how a monthly median of the F2 layer critical frequency (f_oF2) was developed from an extremely large worldwide data base. In fact the gradient map shown in Figure 14 is a result of this work. We have already shown that it is important to include the horizontal gradients of f_oF2 in any analysis and the work by Jones et al is undoubtedly the only satisfactory approach to this problem.

The document by Jones et al describing this work includes a Fortran program which, with monthly coefficients obtainable from NOAA, enables the monthly median value of f_oF2 to be computed above any point in the world at any time. This program was primarily written to accept monthly coefficients using an average sunspot number, but more recent work by Jones & Obitts (Reference 3) has described a more generalized set of coefficients which provides annual continuity and uses more extensive analysis. These generalized coefficients can be obtained from the Ionospheric Prediction Services, NOAA, Boulder, for a sunspot number or a solar flux approach. The value of a monthly median f_oF2 can be computed on a worldwide basis centralized around the specific day in question rather than the 15th of the month; it can also be based on a 12-month running average of solar flux or sunspot number. Private communication with Mrs. Leftin at NOAA indicates that the solar flux approach is likely to provide more accurate values of f_oF2 than the use of the sunspot number.

For the ionospheric profile under discussion, it was decided to use the generalized f_oF2 coefficients from NOAA incorporating solar flux thereby eliminating any need to purchase monthly data from them. The program was made self-contained and enabled a monthly median f_oF2 to be produced above any surface position for any time of day or season and any twelve month running average of solar flux.

The question now arises as to how good these monthly median values are and how much error is introduced by day to day fluctuations. Many daily soundings were analyzed and the monthly median value computed; these were compared with the monthly median predicted values and the actual day to day fluctuations. Some typical results are shown in Figure 15. It is seen that the monthly median predicted values are indeed very close to the actual measured value, but the day to day fluctuations can be as large as $\pm$75%. A technique therefore had to be derived to bring the computed monthly median value closer to the actual value.

It would be pointless to use the daily value of solar flux in the generalized coefficient set which had been built up using a twelve month running average, but it was thought possible that there may be a relation between the difference in f_oF2 from monthly median to daily value and the difference in the 12-month running average of solar flux to the daily value.

Approximately 6,000 real values of f_oF2 from 13 stations widely spread in latitude, longitude, and solar cycle were compared with the predicted values using the NOAA solar flux method. A very surprising result emerged and can be explained by referring to Figure 16. Eliminating the data from stations close to the magnetic poles which did not quite follow the trend of the other stations a comparison between the difference in daily and 12-month flux value and the percentage difference of computed and measured f_oF2 showed all stations having a very similar bias. Figure 16 shows this comparison where the stations having similar latitude were averaged quoting their mean magnetic latitude. The fact that the lines did not pass through the zero points in the graph undoubtedly indicates an erroneous bias in the NOAA predictions, but results help one to update substantially the monthly median f_oF2 value on a daily basis. Further comparisons were carried out with two years of hourly f_oF2 values obtained near solar maximum from Hawaii and the results fit perfectly in the latitude position expected in Figure 16. By these means it is possible to come somewhat nearer the actual daily value of f_oF2. Further accuracy can be derived by update from stations within the general area if this is available and the investigation of this approach will now be explained.

In order to investigate the size of an area from which ionospheric values would show similar deviations from normal, many comparisons of three or more stations were investigated for random dates. It is well known that magnetic disturbances can effect the ionosphere above one station in one direction and a nearby station in an opposite direction. For this reason investigations of disturbances were not carried out near to the magnetic poles. Over 100 groups of stations from various continents and having similar longitudes were compared in similar ways. Figure 17 is a typical result of such a test and shows f_oF2 disturbances being recorded simultaneously at sites 1,000km apart. The percentage error in the predicted f_oF2 value when compared to the real value was noted to be similar in 90% of the cases where stations were within 2,000km of one another in a longitudinal direction and investigations over the 'quiet' North American continent show improvement in 9 out of 10 cases when f_oF2 was updated with information from across the continent; or 3,000 to 4,000km. However, in general, the update procedure is restricted to information from within 2,000km of the evaluating station.

A.1.5 Predicting the Height of the Maximum Layer

In order to predict the real height of f_oF2 the M(3000)F2 predictions from NOAA were used. To explain the terminology:

$$M(3000)F2 = M\ FACTOR = MUF(3000)F2 / f_oF2,$$

where MUF(3000)F2 is the maximum usable frequency to propagate by reflection from the F2 layer a distance of 3,000km. The M(3000)F2 predictions can be calculated on a monthly basis from a generalized set issued by NOAA and provide the monthly median value as a function of sunspot number.

Knowledge of this factor along with the f_oF2 value enables the height of the layer to be calculated using the equations of Appleton & Beynon (Reference 1). If M is the M(3000)F2 factor and one assumes that y_m divided by the height of the bottom edge of the lower layer is greater than 0.4, then it is possible to derive the following polynomial,

$$h_m = 1346.92 - 526.40M + 59.825M^2,$$

where h_m is the required height.

A.2 Model Accuracy

As a means of testing the accuracy of the model, an intense comparison with Faraday rotation data has been performed as well as tests with two frequency data, actual ionospheric profiles, and use in orbit determination programs.

Remarkable improvements have been noticed in precise orbit determination systems and the model has reduced the number of iterations needed for the program to converge as well as the size of the residuals by up to a factor of four. Excellent results have been noted with orbit programs using elevation angle, range and range rate systems.

The most extensive tests were carried out by comparing Faraday rotation data for seven stations from Hawaii to Puerto Rico to Alaska looking at the ATS1, ATS3, and SYNCOM3 satellites. In all, over 100 station months of continuous data were used during the years 1965 and 1967-1969 with data taken every hour. The integrated model data was compared with these actual results; update situations were also investigated. The results are shown in Figure 18 where the percentage of the ionosphere removed with the model is shown. In general, between 75 and 90% of the ionospheric effects are removed and these circumstances are for solar maximum conditions.

References

1. E. V. Appleton & W. J. G. Beynon, Proc. Phys. Soc. 52, Pt. I, 518 (1940); Proc. Phys. Soc. 59, Pt. II, 58 (1947)

2. W. B. Jones, R. P. Graham, M. Leftin, "Advances in Ionospheric Mapping by Numerical Methods," ESSA Technical Report ERL 107-ITS 75, (May 1969)

3. W. B. Jones, D. L. Obitts, "Global Representation of Annual and Solar Cycle Variation of f_oF2 Monthly Median 1954-1958," OT/ITS Research Report No. 3 (Oct 1970)

4. A. N. Kazantsev, Tr. IRE AN SSSR, 2, 36, (1956).

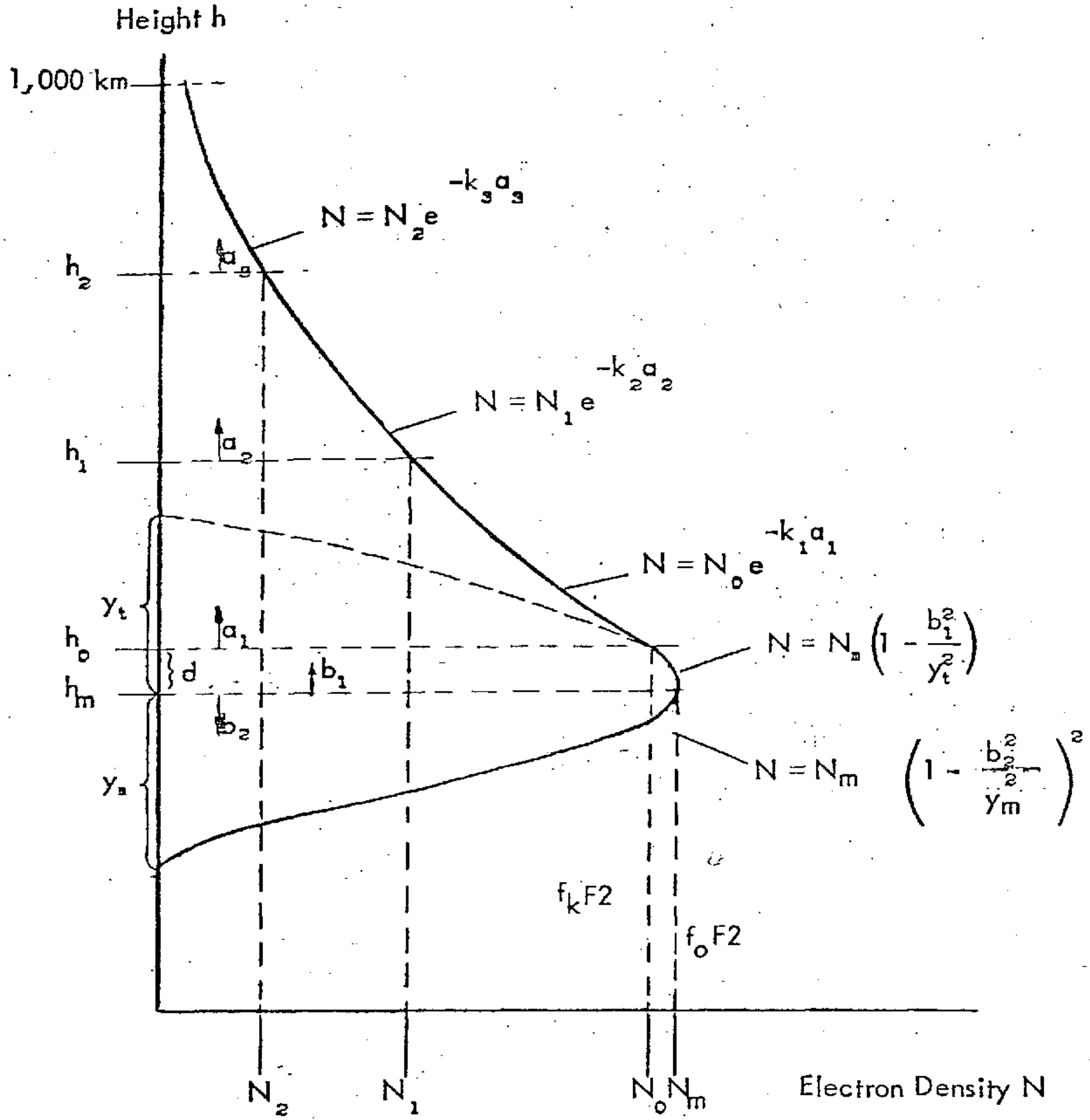

Fig. 7. The Exponential Parabolic & Bi-parabolic Profile

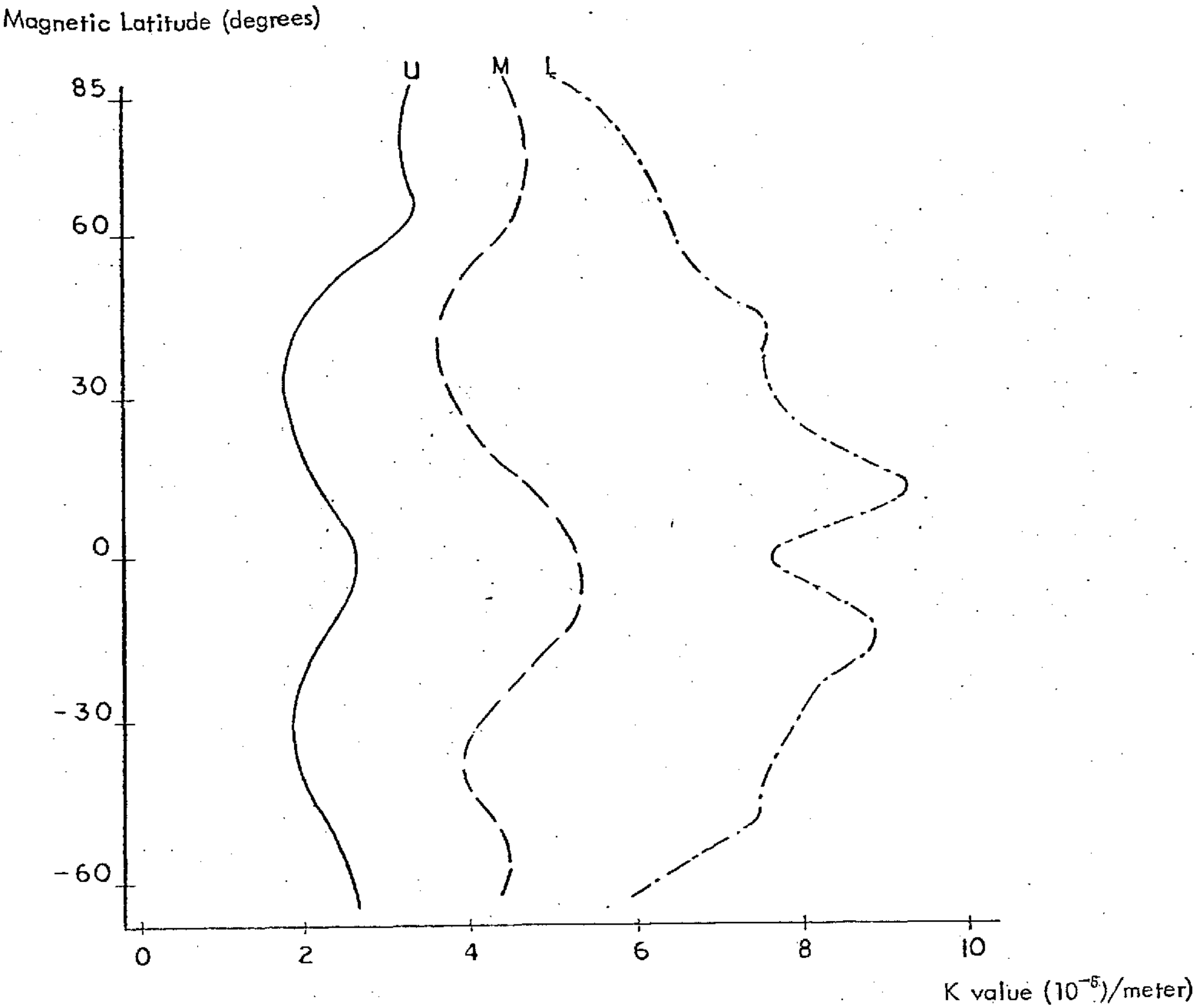

Fig. 8 The mean fluctuation of the decay constant k with magnetic latitude for the upper (U), middle (M) and lower (L) portions of the topside ionosphere.

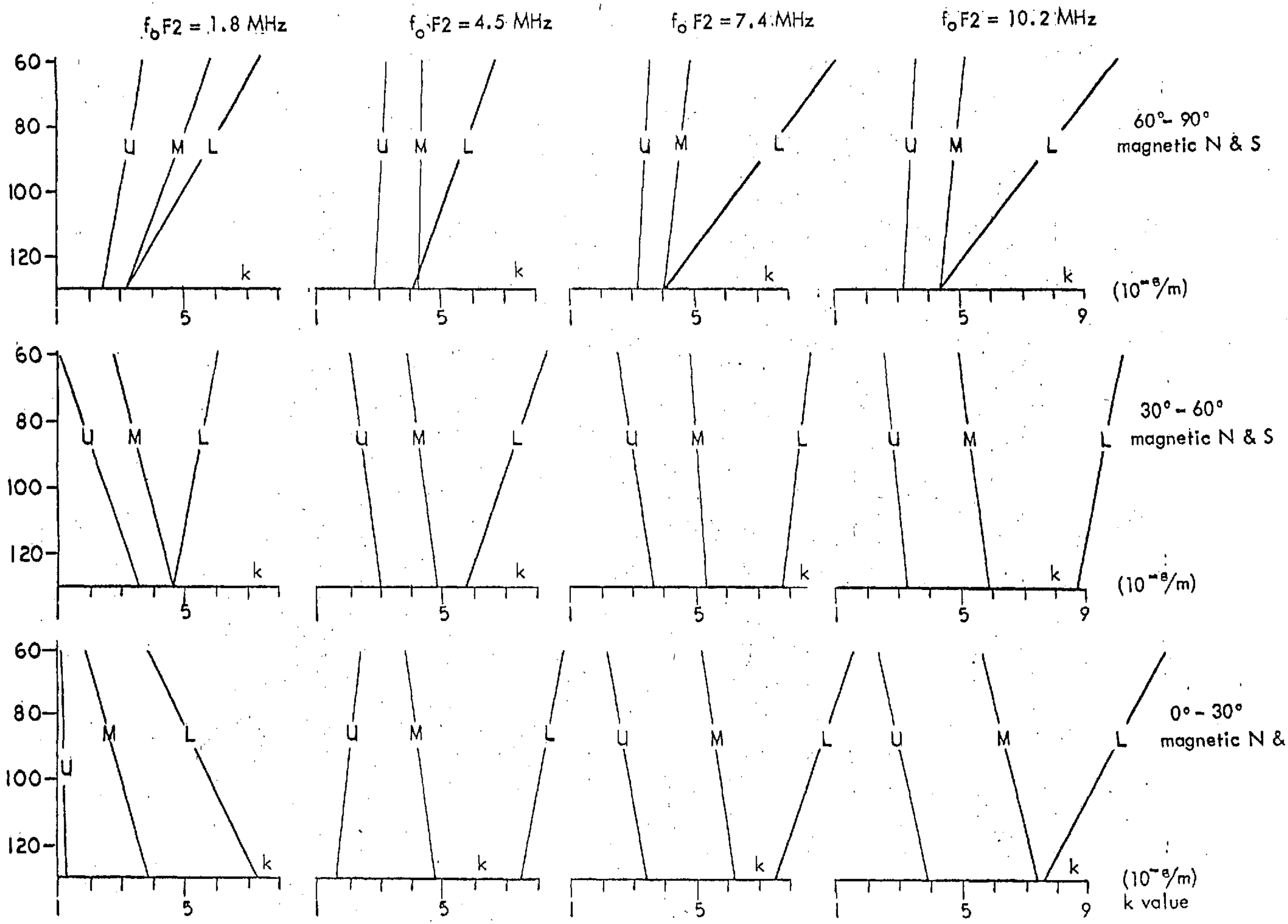

Fig. 9 Variation of k for the upper (U), middle (M) and lower (L) topside profile due to solar flux, f_oF2 and magnetic latitude.

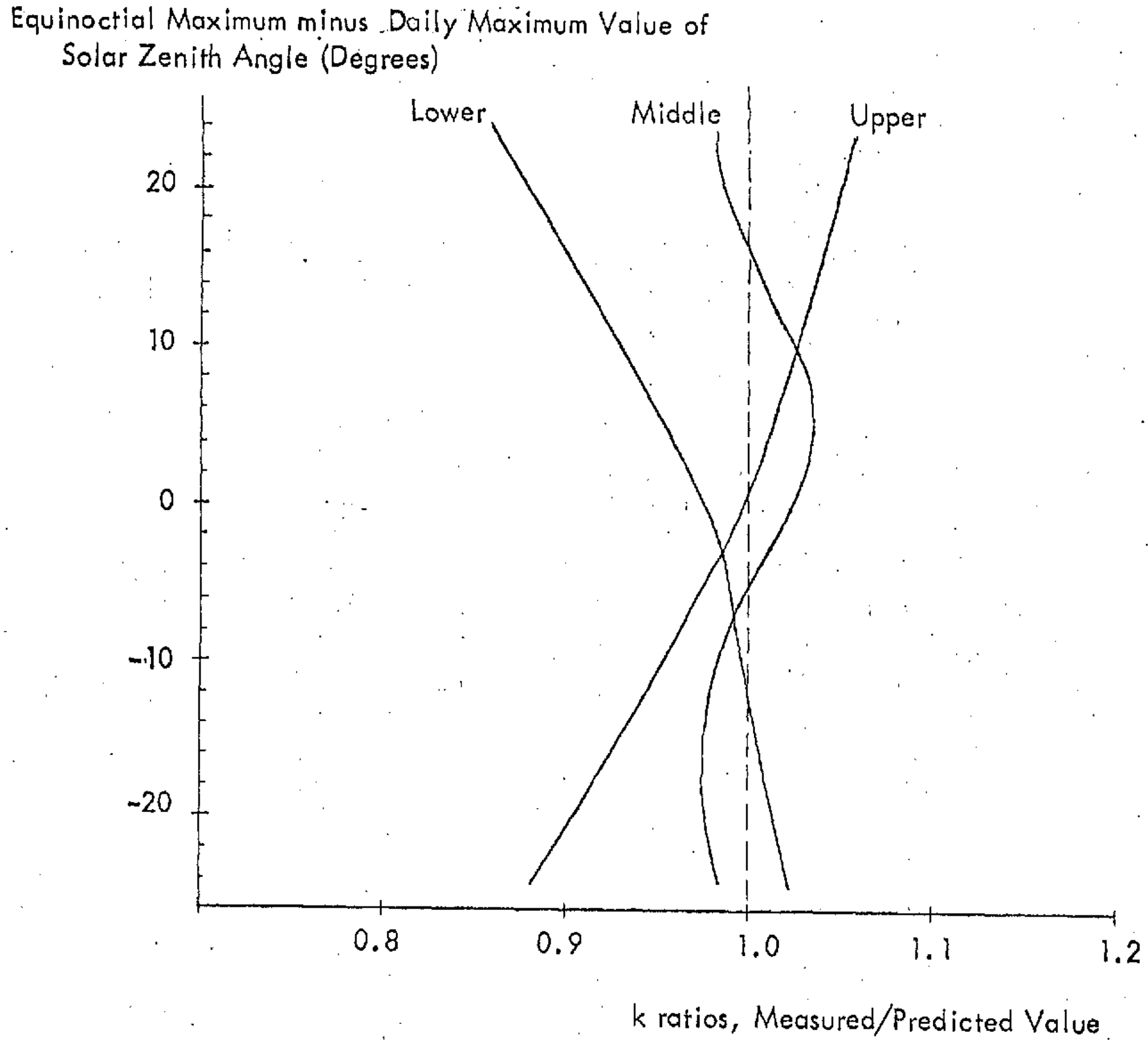

Fig. 10 The seasonal variation in the predicted k values

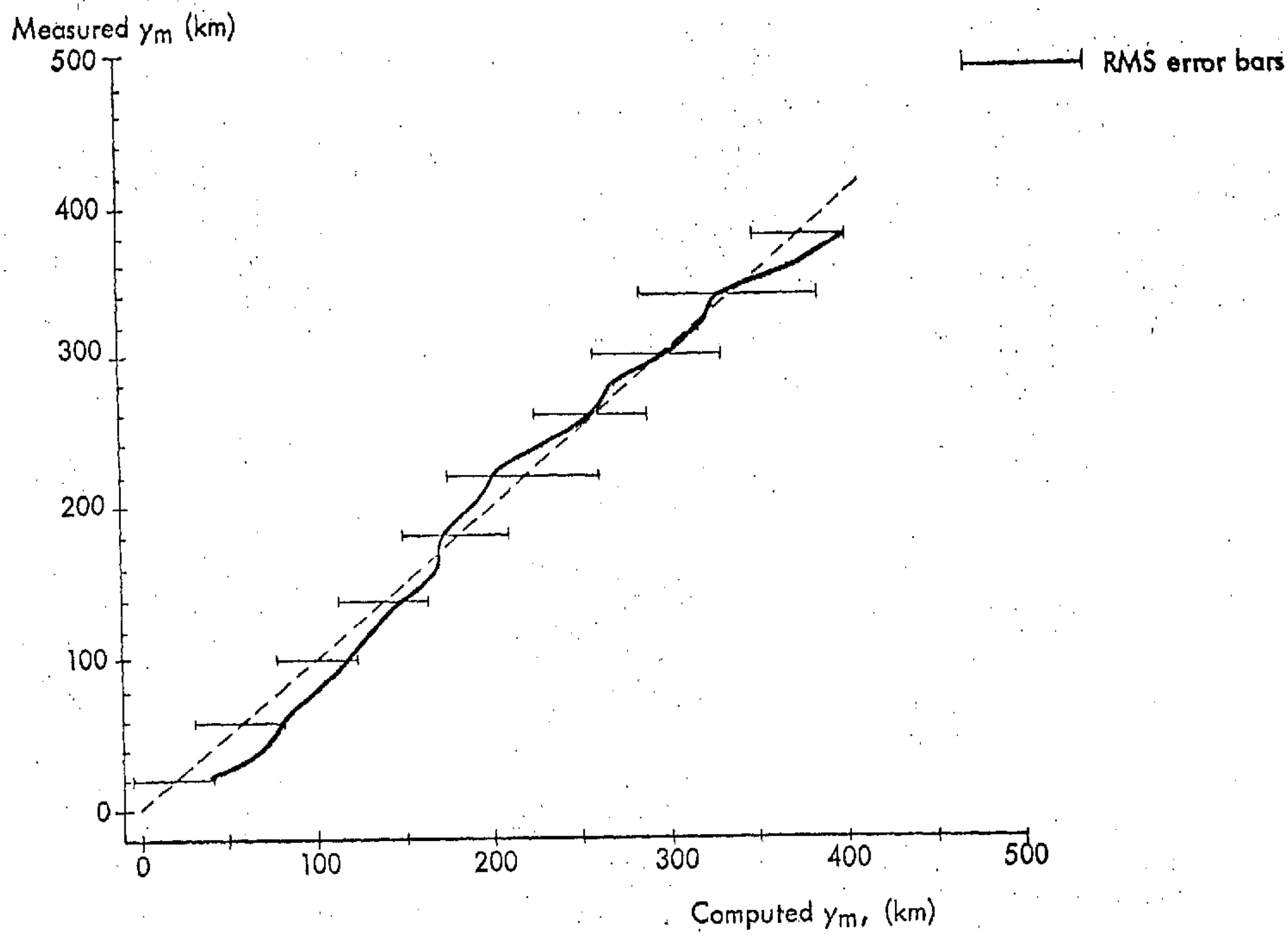

Fig.11 The comparison of measured and predicted y_m for 12,000 profiles showing RMS error bars.

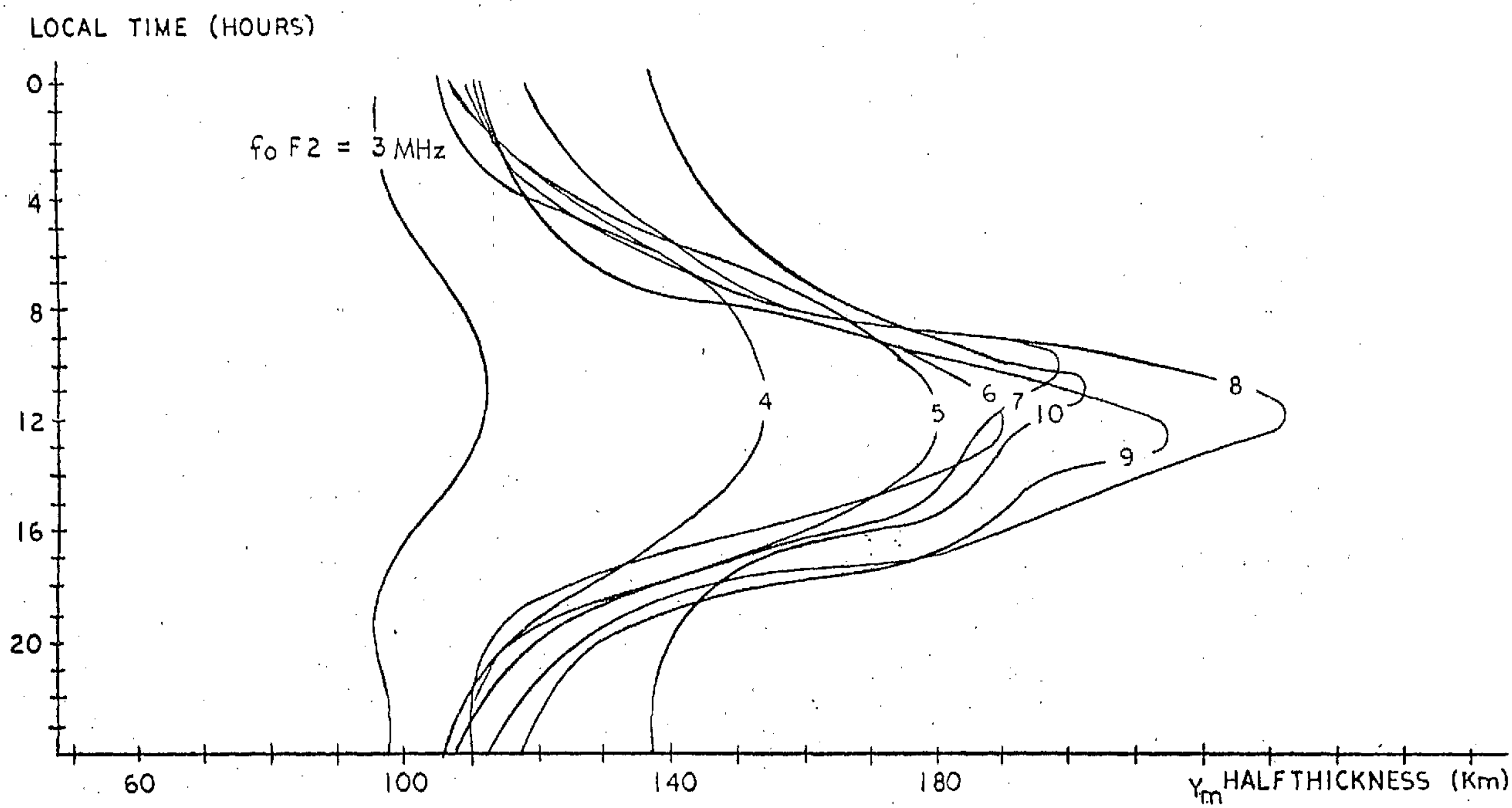

Fig. 12 Variation of y_m as a function of f_oF2 and local time.

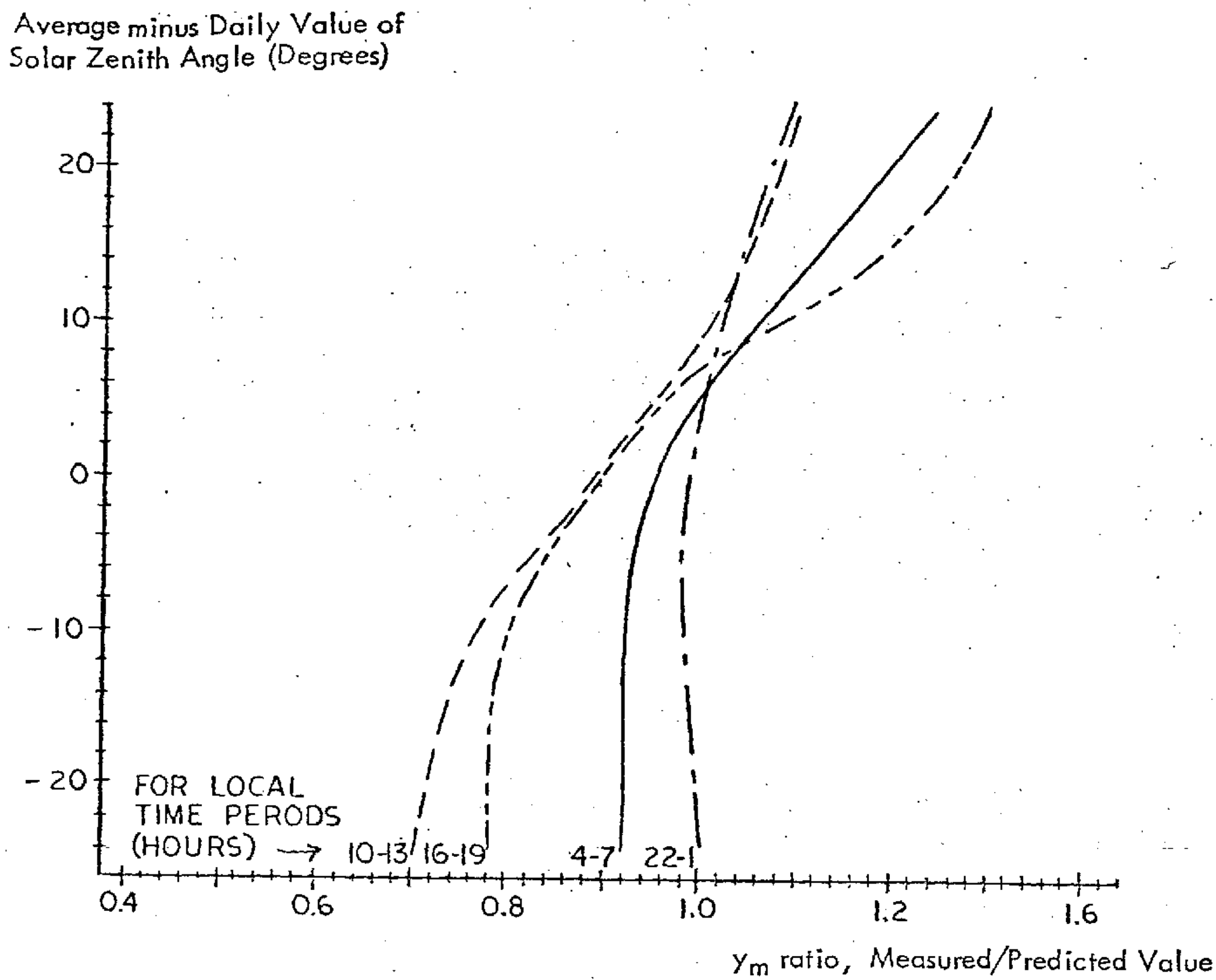

Fig. 13 The seasonal variation of predicted y_m as a function of local time.

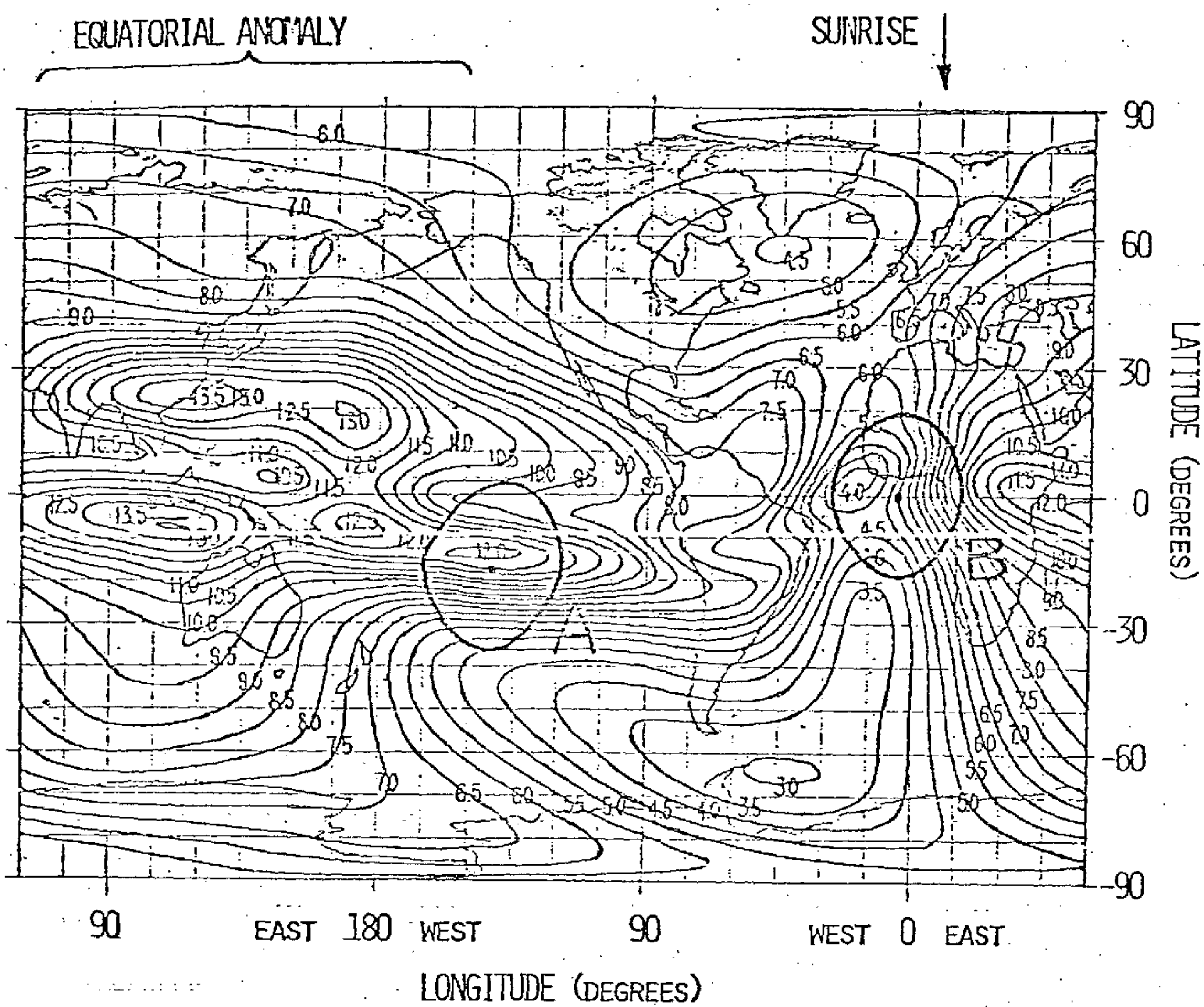

Fig.14 The predicted global status of a monthly median f_xF2 at 6.0 a.m. UT August 1968 showing areas of visibility for two hypothetical ground stations.

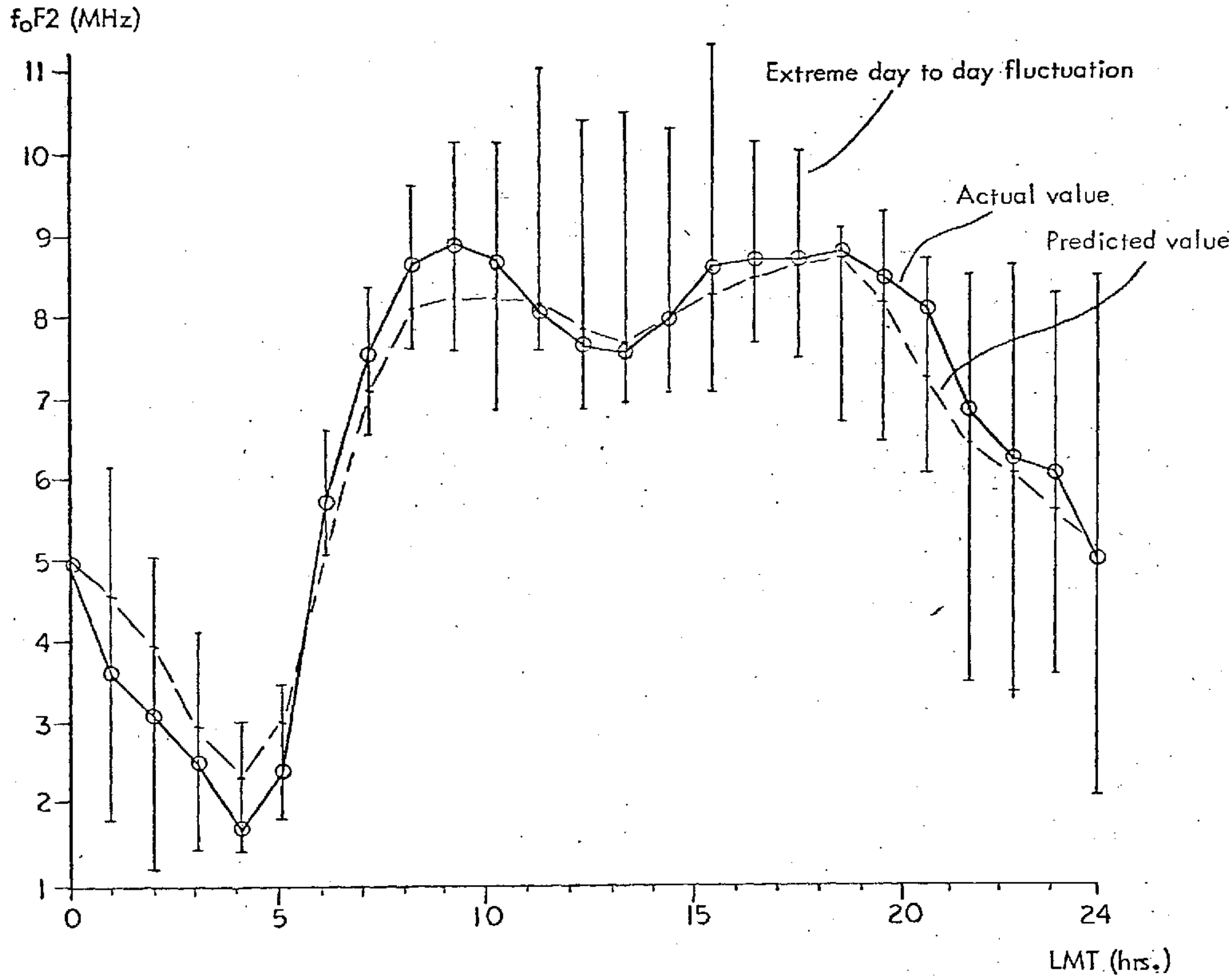

Fig. 15 The predicted and actual monthly median values of f_oF2 for Ibadan June 1962 showing the extreme day to day fluctuations.

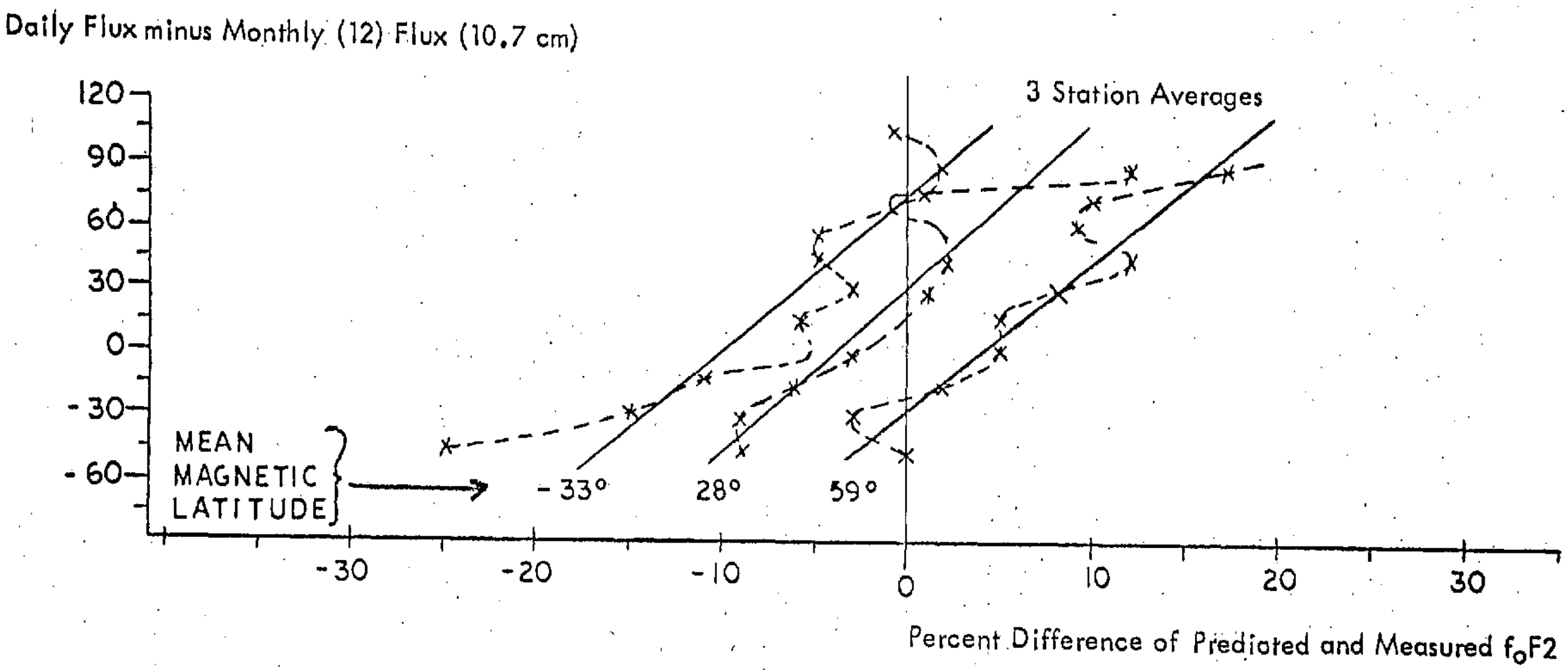

Fig. 16 An error in the NOAA f_oF2 predictions as a function of magnetic latitude and daily solar flux minus the 12 month running average.

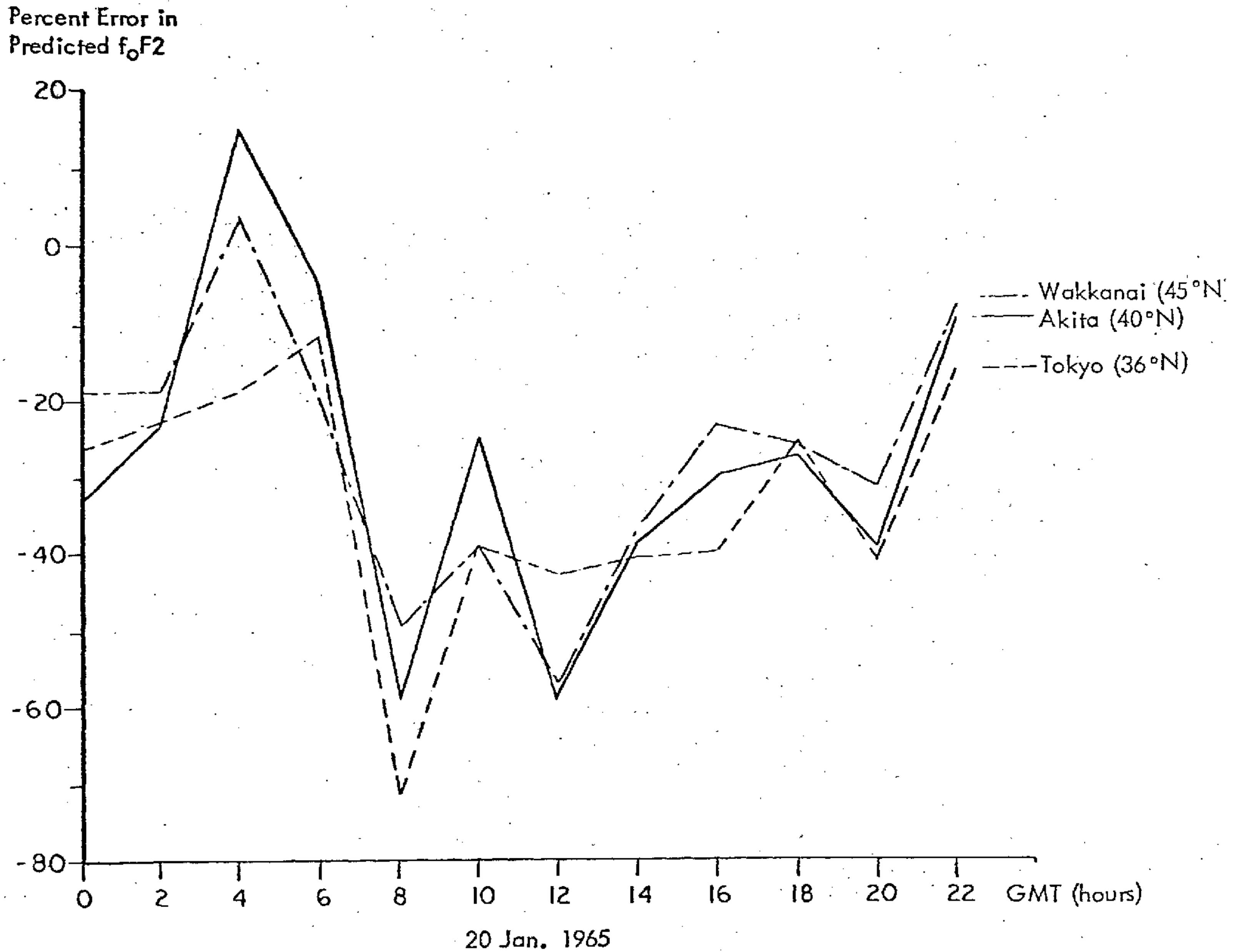

Fig. 17 Deviations in f_oF2 evident over a distance of 1,000 km

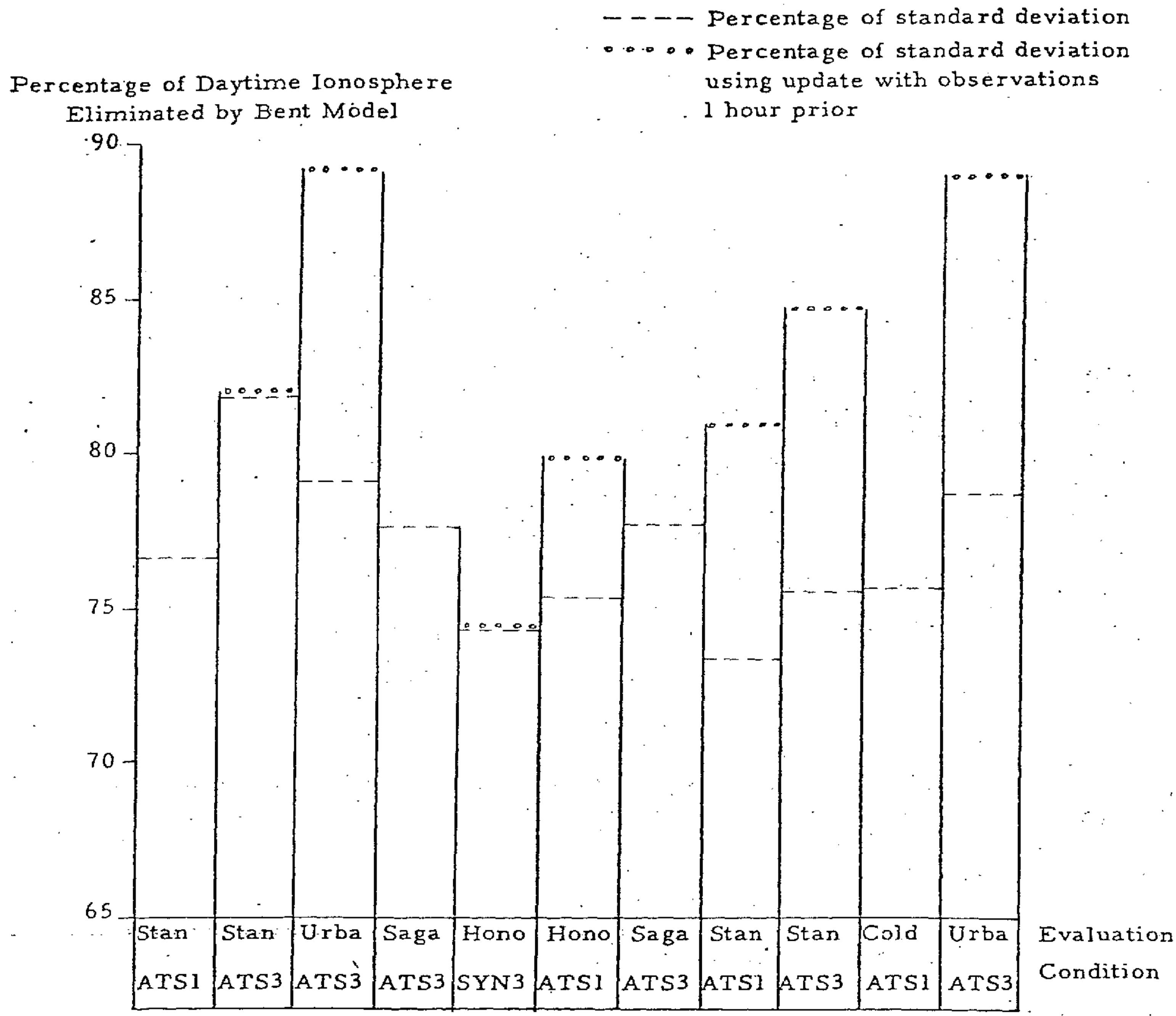

Figure 18 Percentage of Daytime Ionosphere Eliminated for Different Evaluation Conditions

APPENDIX B

B.1 Earth's Magnetic Field Model

The model computes the earth's magnetic field components at a desired location following the spherical harmonic analysis of the magnetic field by Chapman and Bartels (Reference 1) and using the coefficients g_n^m, h_n^m given by Jensen and Cain (Reference 2) for Epoch 1960. The X-north, Y-east, and Z-vertical (up) components of the magnetic field are computed for any location, defined by its latitude ϕ, longitude λ, and height h above the earth's surface. Introducing the colatitude $\varphi=90°-\phi$ and the ratio $R=R_e/(R_e+h)$, where R_e is the radius of the earth, the components X, Y, Z are given by,

$$X = \sum_{n=1}^{6} \left\{ R^{n+2} \sum_{m=0}^{n} \frac{d}{d\varphi} P_{n,m}(\cos\varphi) \left[g_n^m \cos(m\lambda) + h_n^m \sin(m\lambda) \right] \right\}$$

$$Y = \frac{1}{\sin\varphi} \sum_{n=1}^{6} \left\{ R^{n+2} \sum_{m=0}^{n} m\, P_{n,m}(\cos\varphi) \left[g_n^m \sin(m\lambda) - h_n^m \cos(m\lambda) \right] \right\}$$

$$Z = -\sum_{n=1}^{6} \left\{ (n+1) R^{n+2} \sum_{m=0}^{n} P_{n,m}(\cos\varphi) \left[g_n^m \cos(m\lambda) + h_n^m \sin(m\lambda) \right] \right\}$$

The multiple of the associated Legendre function is given by,

$$P_{n,m}(\cos\varphi) = \sin^m\varphi \left[\cos^{n-m}\varphi - \frac{(n-m)(n-m-1)}{2(2n-1)} \cos^{n-m-2}\varphi + \frac{(n-m)(n-m-1)(n-m-2)(n-m-3)}{(2)(4)\ (2n-1)(2n-3)} \cos^{n-m-4}\varphi - \dots \right]$$

References

1. S. Chapman & J. Bartels, "Geomagnetism," Vol II, Oxford at the Clarendon Press (1962).
2. D.C. Jensen & J.C. Cain, "Iterim Geomagnetic Field," J. Geogr. Res., No. 9, 3568-3569 (Aug. 1962)

```
*********************************************
*                                           *
*  CONVERSION FACTORS FOR FARADAY ROTATION DATA  *
*                                           *
*********************************************
```

DATA REDUCTION FOR

```
START TIME      YEAR,MONTH,DAY= 741023, HOUR,MINUTE,SECOND= 184000
STOP  TIME      YEAR,MONTH,DAY= 741030, HOUR,MINUTE,SECOND= 190000
SATELLITE NO    7407070.
RUN ID          0000007467
```

DESCRIPTION OF COLUMNS IN DATA TABLES

```
PASS NO   SATELLITE PASSES NUMBERED FROM THE BEGINNING OF EACH DAY FOR EACH STATION.
GMT       GREENWICH MEAN TIME (HRS,MIN,SEC). IF TIME IS MARKED BY *, DATA BELONGS TO DAY PRIOR.
LAT,LON   LATITUDE, LONGITUDE (DEGREES) WHERE RAY PASSES THROUGH DENSEST PORTION OF IONOSPHERE.
MBAR      MBAR FACTOR (AMPERE-TURNS/M) FOR CONVERSION OF FARADAY ROTATION ANGLES R (DEGREES) TO
          TOTAL VERTICAL ELECTRON CONTENT EC (ELECTRONS/M**2).
          THE CONVERSION EQUATION WITH FREQUENCY F (HZ) AND CONSTANT K=1.699 IS GIVEN BY
          EC = R * F**2 / (MBAR * K).
          IF MBAR IS MARKED BY **, THIS EQUATION WILL NOT HOLD, SINCE ALONG THE PATH THE ANGLE
          BETWEEN THE DIRECTION OF PROPAGATION AND THE EARTHS MAGNETIC FIELD EXCEEDS 89.5 DEG.
          AN ESTIMATE FOR MBAR IS LISTED ONLY IF SUCH CONDITION OCCURS ABOVE 1000 KM HEIGHT.
```

INTASAT SATELLITE TRACKING STATIONS

STATION NAME	LATITUDE	LONGITUDE	STATION NAME	LATITUDE	LONGITUDE (DEGREES)
SAGAMORE HIL	42.6200	289.1799	THULE	76.5000	291.3999
GOOSE BAY	53.3000	299.6699	MOSCOW	55.0000	37.0000
SVERDLOVSK	57.0000	61.0000	TBILISI	42.0000	45.0000
NOVOSIBIRSK	55.0000	83.0000	LOUVAIN	50.8000	4.4000
FLORENCE	43.8100	11.2100	CALCUTTA	22.9700	88.5000
BOULDER	40.0000	255.0000	DELAWARE	42.8600	278.6099
TORTOSA	40.8000	0.5000	GILLERSHEIM	51.6228	10.0897
IBADAN	7.4300	3.9000	ISTANBUL	41.1300	29.0300
BRISBANE	-27.5000	153.0000	ABERYSTWYTH	52.4200	355.9500
GRAZ	47.0800	15.5000	RUDE SKOV	55.8400	12.4600
NARSSARSSUAQ	61.1700	314.5698	TUCUMAN	-26.9000	294.5999
S.J.DOS CAMP	-23.3000	314.2000	BOCHUM	51.4286	7.1917
NAIROBI	-1.3300	36.8100	PANSKA VES	50.5300	14.5700
NEW DELHI	28.6300	77.2200	OULU	61.1000	25.4800
HONGKONG	22.2000	114.1000	BALI	-9.0000	114.0000
URBANA	40.0690	271.7749	MALINDI KENY	-2.9800	40.1700
ADELAIDE	-35.0000	138.0000	NEUSTRELITZ	53.2800	13.0800
AHMEDABAD	23.0000	72.6000	TIRUCHIRAPAL	10.8200	78.7000
GULMARG	34.0300	74.1100	BELSK	51.8400	20.7900
EL ARENOSILO	37.0990	6.4300			

Header page

ORIGINAL PAGE IS OF POOR QUALITY

*********** STATION= S.J.DOS CAMP YEAR= 74 MONTH= 10 DAY= 26 ***********

PASS NO	GMT HHMMSS	LAT DEGREES	LON DEGREES	MBAR AMP-TURN/M	PASS NO	GMT HHMMSS	LAT DEGREES	LON DEGREES	MBAR AMP-TURN/M	PASS NO	GMT HHMMSS	LAT DEGREES	LON DEGREES	MBAR AMP-TURN/M
1	*234000	-38.0	320.5	24.3586**	2	13400	-40.5	311.0	23.7403**	3	84500	-26.8	330.9	0.0 **
1	*234100	-35.3	319.4	24.9280**	2	13500	-38.0	310.3	23.9093**	3	84600	-28.0	329.7	0.0 **
1	*234200	-33.0	318.5	24.0129**	2	13600	-35.8	309.8	23.0705	3	84700	-29.2	328.6	0.0 **
1	*234300	-31.1	317.7	21.8354	2	13700	-33.8	309.3	21.3218	3	84800	-30.4	327.7	0.0 **
1	*234400	-29.5	317.1	18.6829	2	13800	-32.2	308.9	18.8852	3	84900	-31.6	326.9	0.0 **
1	*234500	-28.1	316.7	14.9719	2	13900	-30.7	308.5	15.9098	3	85000	-32.9	326.1	20.8022**
1	*234600	-27.0	316.3	11.0678	2	14000	-29.5	308.1	12.5473	3	85100	-34.4	325.5	22.0958**
1	*234700	-26.0	315.9	7.1449**	2	14100	-28.3	307.7	8.9270**	3	85200	-35.9	324.9	23.0001**
1	*234800	-25.2	315.6	3.2973**	2	14200	-27.3	307.2	5.1876**	3	85300	-37.7	324.2	23.4722**
1	*234900	-24.4	315.4	0.0 **	2	14300	-26.3	306.7	0.0 **					
1	*235000	-23.6	315.1	4.3316	2	14400	-25.3	306.0	2.5803					
1	*235100	-22.8	314.9	8.1569	2	14500	-24.2	305.3	6.5469					
1	*235200	-22.0	314.7	12.0733	2	14600	-23.1	304.4	10.5344					
1	*235300	-21.2	314.4	16.1380	2	14700	-21.9	303.4	14.4654					
1	*235400	-20.2	314.2	20.3931	2	14800	-20.6	302.3	18.1654					
1	*235500	-19.1	313.9	24.8409	2	14900	-19.0	301.0	21.3193					
1	*235600	-17.8	313.6	29.3793	2	15000	-17.2	299.5	23.8227					
1	*235700	-16.3	313.2	33.7128	2	15100	-15.2	298.1	25.8418					
1	*235800	-14.4	312.7	37.4319										
1	*235900	-12.3	312.2	40.4527										
1	0	-9.8	311.6	42.9262										
1	100	-7.2	310.9	44.8389										
4	102900	-9.4	324.2	33.6318	5	122300	-7.3	310.1	46.3467	6	224300	-35.3	324.8	21.8350**
4	103000	-12.2	322.8	32.2018	5	122400	-9.8	309.9	44.6551	6	224400	-33.0	323.6	21.8662**
4	103100	-14.5	321.6	29.7540	5	122500	-12.1	309.8	42.1648	6	224500	-31.0	322.6	20.7119**
4	103200	-16.5	320.6	26.4740	5	122600	-14.2	309.7	39.0579	6	224600	-29.3	321.7	18.4534**
4	103300	-18.1	319.7	22.7343	5	122700	-16.0	309.7	35.4017	6	224700	-27.9	321.0	15.3603**
4	103400	-19.4	318.9	18.8843	5	122800	-17.5	309.6	31.3837	6	224800	-26.7	320.5	11.7944**
4	103500	-20.5	318.3	15.1229	5	122900	-18.9	309.6	27.2270	6	224900	-25.6	320.1	0.0 **
4	103600	-21.5	317.8	11.5269	5	123000	-20.0	309.5	23.0665	6	225000	-24.6	319.7	0.0 **
4	103700	-22.3	317.4	8.0996	5	123100	-21.1	309.4	18.9600	6	225100	-23.7	319.4	0.0 **
4	103800	-23.0	317.0	4.8067	5	123200	-22.1	309.2	14.9148	6	225200	-22.8	319.2	3.8363
4	103900	-23.8	316.7	1.5978	5	123300	-23.0	309.0	10.9069	6	225300	-21.9	319.0	7.8806
4	104000	-24.5	316.4	0.0 **	5	123400	-24.0	308.8	6.8990	6	225400	-20.9	318.9	12.0226
4	104100	-25.2	316.1	4.8116**	5	123500	-24.9	308.5	2.8545	6	225500	-19.9	318.8	16.2847
4	104200	-26.0	315.8	8.0681**	5	123600	-26.0	308.1	0.0 **	6	225600	-18.7	318.8	20.6583
4	104300	-26.8	315.6	11.4525	5	123700	-27.1	307.7	5.4544**	6	225700	-17.3	318.8	25.0680
4	104400	-27.8	315.3	14.9480	5	123800	-28.4	307.1	9.6530**	6	225800	-15.7	318.8	29.3329
4	104500	-29.0	315.0	18.5101	5	123900	-29.9	306.5	13.7672**	6	225900	-13.8	318.8	32.9937
4	104600	-30.3	314.7	22.0101	5	124000	-31.6	305.6	17.5771**	6	230000	-11.5	318.8	35.7117
4	104700	-32.0	314.2	25.1961	5	124100	-33.5	304.7	20.7698**	6	230100	-9.0	318.8	37.6767
4	104800	-34.0	313.7	27.6798	5	124200	-35.8	303.5	22.9912**	6	230200	-6.3	318.6	39.0737
4	104900	-36.4	313.1	29.0179**										
4	105000	-39.2	312.2	28.9355**										

ORIGINAL PAGE IS OF POOR QUALITY

Data Page. The flags in the GMT and MBAR columns are explained in Section 2.